An Empirical Potential for Hydrogen Bond Energies

Determination of the Orientation of Anthracene Molecules in the Unit Cell by means of a Refractivity Method

Some Ab Initio Calculations Involving Acetonitrile Exchange Reaction

by

Szu-Lin Chen

Dissertation submitted to the Faculty of the

Virginia Polytechnic Institute and State University

in partial fulfillment of the requirements for the degree of

Doctor of Philosophy

in

Chemistry

APPROVED:

Jimmy W. Viers, Chairman

John C. Schug

James P. Wightman

Brian E. Hanson

Gerald V. Gibbs

May, 1987

Blacksburg, Virginia

An Empirical Potential for Hydrogen Bond Energies

Determination of the Orientation of Anthracene Molecules in the Unit Cell by means of a Refractivity Method

Some Ab Initio Calculations Involving Acetonitrile Exchange Reaction

by

Szu-Lin Chen

Jimmy W. Viers, Chairman

Chemistry

(ABSTRACT)

Topic I

An empirical potential for calculating hydrogen bonding energies is developed for systems of the type A-H--B, where A and/or B is oxygen or nitrogen. Point charge and van der Waals interaction are included in the potential. The parameters of the potential were optimized by means of a simplex algorithm within a range of A-B distances from 2.8 A through 5.0 A. The root mean square deviation between the empirical potential and the ab initio results of 216 configurations of $(H_2O)_2$, $(NH_3)_2$ and $NH_3 \bullet H_2O$ is 0.9 kcal/mol and 0.5 kcal/mol for 61 configurations of methanol dimers. Applications of the potential to water dimers, ammonia dimers, their mixed dimers, water oligomers and ice-h as well as the β form of the methanol crystal show that the potential yields reasonable results compared to those computed by "ab initio" methods using 6-31G* basis sets. The potential is compatible with MM2 program. It is simpler than earlier potentials in that neither dipoles nor Morse potentials are involved. It should be superior to the empirical potentials developed by Jorgensen that used STO-3G ab initio calculated results as the standards. The potential might be useful for estimation of hydrogen bond energies in a local part of a large molecule to avoid the prohibitive expense of ab initio calculation.

Topic II

The monoclinic anthracene crystal is used as an example to demonstrate the feasibility of optimizing the orientation of molecules in the unit cell by matching calculated and experimental refractivity ellipsoids using a simplex algorithm. The calculated refractivity ellipsoid is determined by use of an empirical formula using bond directional polarizabilities. Optimization of the molecular orientations to provide the best fit to the experimental ellipsoid starting from several assumed orientations results in fits for which the maximum deviation from the experimental molecular orientation was no more than 10 degrees. The method can be applied to other monoclinic molecular crystals directly and could be extended to other crystal systems with anisotropic optical properties.

Topic III

Three mechanisms (Walden inversion, addition-rearrangement-elimination and proton 1,3 shift mechanisms) of the following reaction were suggested by Jay et al. and Andrade et al. respectively.

$$CH_3CN + \overset{*}{C}N^- = CH_3\overset{*}{C}N + CN^-.$$

The mechanism of Walden inversion was determined to be the least likely one based on Andrade's MNDO results. Our calculations, based on 3-21G and 4-31G results, show the contrary result that the Walden inversion is the most likely mechanism among the three considered. However, solvation effects were neglected in the calculations and these effects could play a major role in the choice of mechanisms. Simple calculations based on Boltzmann distribution of precusor concentrations and the Arrhenius law show that Walden inversion predominates over Jay's addition-elimination-rearrangement mechanism even when MNDO energy levels were used. Estimated orders of magnitude for the rate ratios were determined.

Acknowledgements

The author is indebted to Dr. Jimmy W. Viers and Dr. John C. Schug for their guidance during the period of his graduate study at Virginia Tech (VPI & SU). Their instruction and encouragement made the appearance of the second part of the dissertation in Acta Cryst., A42, 137-9 (1986) possible, and made the presentation of the first part available at the ACS regional meeting. He is grateful to Dr. Wightman, Dr. Hanson and Dr. Gibbs for their advice during the preparation of the current dissertation. Since Dr. Alan F. Clifford (the former Dept. Head) and Dr. James Wolfe (the Dept. Head) accepted him as a graduate student, their encouragement and support made his continuous study possible. Dr. J. D. Graybeal (the associate Dept. Head) provided the author assistance in his study toward the degree. The appearance of this dissertation is the result of encouragement and help from all of them.

Table of Contents

List of Illustrations

List of Tables

General Introduction

The thesis is composed of three topics. The first is the study of an empirical potential for calculating hydrogen bonding energies for systems involving oxygen and/or nitrogen. One purpose for empirical potentials of this type could be to apply it to interaction involving large molecules such as polypeptides and amino acids, where H-bonds are involved, for example, the hydrogen bonding interaction in adenine-thymine and guanine-cytosine. Before the potential can be used for purposes such as this, it is necessary to test the potentials for a variety of small molecular configurations. As shown in the thesis, we have obtained reasonable results for small molecular configurations, ice-h and methanol crystal when the potential parameters were optimized based on 6-31G* basis computations of 216 configurations of water, ammonia and mixed dimers. For large molecules, it might be better to optimize the parameters based on crystal data as was done by Hagler.[1] The empirical H-bonding potential can also be applied to liquid simulation studies. Jorgenson[2] has recently developed 12-6-3-1/12-6-1 potentials which he has used for liquid simulation studies.

Taylor[3a] developed a potential based on a dipole-dipole model to study carbohydrates. Kroon-Batenburg et al.[4] improved Taylor's potential especially in the bifurcated H-bonding configurations of small molecules. An extra repulsive term was added to Kroon's potential and was shown to play an important role to improve the energies of bifurcated configurations. In order to avoid the point charge overlap catastrophe, switch functions have been used in Ben-Naim-

Stillinger's potential.[5] Our potential could also benefit from the use of the extra repulsive terms and switch functions. We leave those improvements for future work.

In the second topic of the thesis, we have demonstrated the feasibility of optimizing the orientation of an anisotropic molecule such as anthracene in its crystal cell by means of fitting the directional refractivities of the molecule and that of the crystal. It might be useful as one of auxiliary methods for crystal structure determination. It may also be useful in studies of liquid crystals.

In the third topic, we support the Walden inversion as the most likely mechanism for acetonitrile exchange reaction through ab initio calculations and simple kinetic calculations. An addition-rearrangement-elimination mechanism was suggested by Jay et al.[6] and 1,3 hydrogen shift in solution was suggested by Andrade et al..[7] Our results are contrary to both Jay's and Andrade's results.

An Empirical Potential for Hydrogen Bond Energies

Introduction

Morokuma et al.[8], Bene et al.[9] and Kollman et al.[10a] have applied ab initio calculations to determination of the structure of the water dimer. The accuracy of the ab initio calculation of bond lengths and bond angles now approach 0.02 A and 3 degrees, respectively, for small molecules.[11] This makes the determination of molecular geometry possible where experiments are difficult or even impossible to perform, such as the study of transition state structures.

However, it is prohibitively expensive to perform ab initio calculations to determine intermolecular interaction energies of large monomers, simulations of liquid structure and estimates of lattice energy based on H-bonding interactions. In some cases, such as biochemical molecules, it is not possible at present to apply ab initio calculations. Empirical potentials provide useful alternatives. For example, Jorgensen[2,12a] determined empirical potentials by fitting ab initio (STO-3G) SCF calculations on water, ammonia and methanol dimers, and then employed them in performing Monte Carlo simulations of the liquid states of these materials.

In this thesis we developed an empirical potential which is aimed at fitting the hydrogen bonding energies to ab initio results based on calculations which we performed using 6-31G* basis sets and on MCYs' CI calculations.[13] The fitting range chosen is for O-O distances from 2.8 A to 5.0 A. This is within the most difficult range to determine the interaction energies of two water

molecules.(page 239 of Ref. 14) The parameters involved in the empirical potential were optimized using a simplex optimization method.[15] The potential should be applicable to A-H--B systems where A and B are either O or N. We applied the potential to $(H_2O)_2$, $(NH_3)_2$, $NH_3 \bullet H_2O$, some water oligomers, ice-h and methanol crystal. The potential should also be valuable in the estimation of H-bonding energies, virial coefficients and configuration integration as well as in liquid simulation where H-bonding is involved.

Historical background

Stockmayer[16] suggested a potential energy function between a pair of similar polar molecules. It is composed of inverse power repulsion, inverse power attraction and permanent dipole-dipole interaction:

$$U = lr^{-s} - cr^{-6} - m^2 r^{-3} g$$

where s > 6, m is the permanent dipole moment, g = 2cos A cos B - sin A sin B cos C, A and B are the inclinations of the two dipole axes to the intermolecular axis, and C is the azimuthal angle between them. He applied the potential to water and ammonia, and calculated reasonable values of the second Virial coefficients using both this potential and a hard sphere potential with an adjusted parameter. The differences between the observed and the calculated second virial coefficients of ammonia and water are less than 3.5 cc/mol within the temperature range of 250K through 750K when the diameters of the impenetrable spheres are 3.18A (ammonia), 3.16A (water) for hard sphere models and 2.76A for a inverse-power model of water. Rowlinson has used the Stockmayer potential to calculate the second and third virial coefficients for water vapor.[17] The interactions involved are mainly hydrogen bonding energies. However, Hagler showed that the Stockmayer potential does not fit the crystal data satisfactorily.[1] The aptness of the Stockmayer potential for understanding condensed phases is questionable in that the minimum energy for a set of point

dipoles is attained in the hexagonal close-packed crystal, not the tetrahedrally coordinated ice lattice. In the wide variety of hydrate crystals loosely termed "clathrates", the water molecules stoutly maintain the local tetrahedral coordination observed in ordinary ice.[5]

Hagler[1] suggested an amide hydrogen potential involving inverse sixth power attraction, inverse power repulsion, partial charge coulomb interactions and a Morse potential term as the covalent part of the hydrogen bond term. Attenuation of the Morse potential is accomplished by an exponential angular dependence factor. All the parameters were fitted to experimental crystal data using least-squares fitting.

Jorgensen[2,12a] fitted his potentials to STO-3G SCF results for Monte Carlo simulation of water, ammonium and methanol liquids. Those potentials are based on point charge models. He used 12-6-3-1 potential functions for water and ammonia dimers and a 12-6-1 potential function for the methanol dimer. (Recently he fitted his potential parameters to the experimental data for sulfur compounds.[12b])

In order to simulate the geometries of carbohydrates, Taylor[3a,3b] developed a potential for the O-H--O hydrogen bond where the electrostatic component is calculated from the classical Jeans equation for dipole-dipole interactions; Hill's equation is used for the van der Waals component; an attenuation factor and van der Waals properties of the lone pairs are explicitly taken into account; and a Morse component and its attenuation factor are involved in the potential. Taylor's potential is compatible with Allinger's molecular mechanics program (MMI).[18a] This potential yielded good results for water oligomers. However, it is suitable only for O-H--O bonds, and it is unnecessarily complicated. Kroon-Batenburg and Kanters[4] developed an empirical O-H--O hydrogen bond potential for MM2 force field calculations. Some modifications of the parameters were made to the MM2 force field and an extra exponential term was added in order to improve the bifurcated interaction of water dimers.

A point charge model was adopted by Popkie et al.[19] to find an analytical expression which is similar to that proposed by Bernal and Fowler.[20] The parameters involved were optimized to fit the Hartree-Fock energies. A potential surface was calculated and compared to the surfaces based on Rowlinson's[17] and Ben-Naim & Stillinger's potential.[5] A Monte Carlo simulation of liquid water where 27 or 64 molecules of water were involved was performed using Popkie's potential.[19] The results were in good agreement with the experimental data for liquid water, except that the second peak of the radial pair correlation function for oxygen-oxygen was not obtained.

Based on Bjerrum's four-point-charge model of the water molecule,[21] Ben-Naim and Stillinger suggested a tetrahedral charge model for the water molecule.[5] The potential is composed of two parts: the coulomb interactions among point charges between the different water molecules and the Lennard-Jones 12-6 interactions. The coulomb term contains a switch factor with two distance parameters, R and R′, to avoid the charge overlap catastrophe. The distances of the charges from the centeral oxygen nucleus was chosen to be 1.0A. The parameters of the Lennard-Jones potential used were the same as for neon. The absolute charge quantity is kq, where q is the electron charge and k is a parameter. When $k = 0.17$, the known dipole moment for the free water molecule was reproduced. When $k = 0.19$ and the other two parameters, R and R′, were chosen to be 2.0379A and 3.1877A, the energies of the water dimers with 2.76A between two oxygens were as follows:

Symmetrical eclipsed	-6.50 kcal/mol
Nonsymmetrical eclipsed	-5.58 kcal/mol
Symmetrical staggered	-5.34 kcal/mol
Nonsymmetrical staggered	-6.13 kcal/mol.

These data are compared with our results in Table 10.

Other empirical models suggested for intermolecular interactions between water monomers also have been suggested.[14,22] In general, point charge models have been shown to produce reasonable results without complicated calculations. Among these were Verwey (1949), Pople (1951), Bernal and Fowler (1933), Rowlinson (1951), Bjerrum (1951), Campbell (1952), and Cohan et al. (1962).[22] The parameters they designed were adjusted to fit the experimental dipole moment. A multipole-

expansion model was suggested by Coulson and Eisenberg (1966).[22] Construction of a hydrogen bonding potential by Gaussian functions was also suggested.[14] In an empirical potential suggested by Oies et al.,[23] a "switch distance" of 3.3 A was adopted to distinguish a hydrogen bond from a van der Waals interaction. When the distance is less than 3.3 A, the interaction is treated as a hydrogen bonding, otherwise it is considered as a van der Waals interaction.

Application of empirical potential to the calculations of various water oligomers have also been carried out.[3,5,14]

A variety of ab initio[9,24,25] and empirical and semi-empirical methods[3,22,26] have also been used to calculate H-bonding energies of water oligomers and the lattice energies of ice-h.

Research methods

Standards for fitting

Dimerization energies of 216 configurations, calculated using ab initio methods, were adopted as standards for fitting the parameters of our empirical potential. Among the 216 configurations, 61 configurations of water dimers $(H_2O)_2$ were calculated by Matsuoka et al.[13]. We computed dimerization energies for 85 configurations of the ammonia dimers $(NH_3)_2$ and 70 configurations of the mixed dimers $NH_3 \bullet H_2O$ using 6-31G* basis sets. The configurations of the ammonia dimers and mixed dimers are shown in Figure 1 and Figure 2. The 6-31G* basis set was chosen based on the comparison of the results from Allen as well as calculations we performed using 4-31G, 6-31G* and 6-31G** basis sets as shown in Figures 3 and 4. In both figures, curves C (using 6-31G*) and B (using 6-31G**) show nearly the same energies. But computations using the 6-31G* basis is less expensive than that using the 6-31G** basis set. Curve S (STO-3G) is quite different from the others in shape as well as in energies. This suggests that the results based on the STO-3G basis set used by Jorgensen[2,12a] are likely not suitable as criteria for standards. These ab initio results are listed in Tables 1-3.

Optimization method - simplex algorithm

By means of a fortran program "All", written by Viers and Schug, combined with a simplex algorithm[15], we optimized the parameters, namely the charges and their locations in the monomer, by fitting the calculated empirical energies to the cited ab initio results for the 216 dimer configurations. A function FN to be optimized to a mininum value was shown as follows:

FN = (61 x BESD of water dimers + 75 x BESD of ammonia dimers + 70 x BESD of mixed dimers)/216.

where the weighting factors, 61, 75 and 70, are the numbers of the configurations for each kind of dimers. The BESD is the best estimate of the standard deviation as follows:

$$BESD = \sqrt{\Sigma(Ei - Eab)^2/(n - 1)}$$

where n is the number of configurations, i.e. 61, 75 or 70 in each kind of dimers; Eab is the energy of the ab initio result for each configuration and is considered as the "true" value; Ei is the calculated empirical result for the same configuration. The monomer geometries of H_2O and NH_3 involved in the optimization are the optimized geometrical results obtained from ab initio calculations using 6-31G* basis sets. For simplicity, it is assumed that the monomers retain their geometry in their dimers or oligomers.

Linear types: B, B1, B2
Bifurcated types: A, A1, A2
Cyclic types: D, D1

	θ (deg)	φ (deg)
A	0.	-
A1	0.	-
A2	0.	-
B	68.3	0.
B1	68.3	0.
B'	68.3	30, 60, 90
B2	52.8	0.
C	90.	0.
C1	90.	0.
C'	90.	30, 60, 90
D	128.5	0.
D1	128.5	0.
D11	128.5	0.
D'	128.5	30, 60, 90

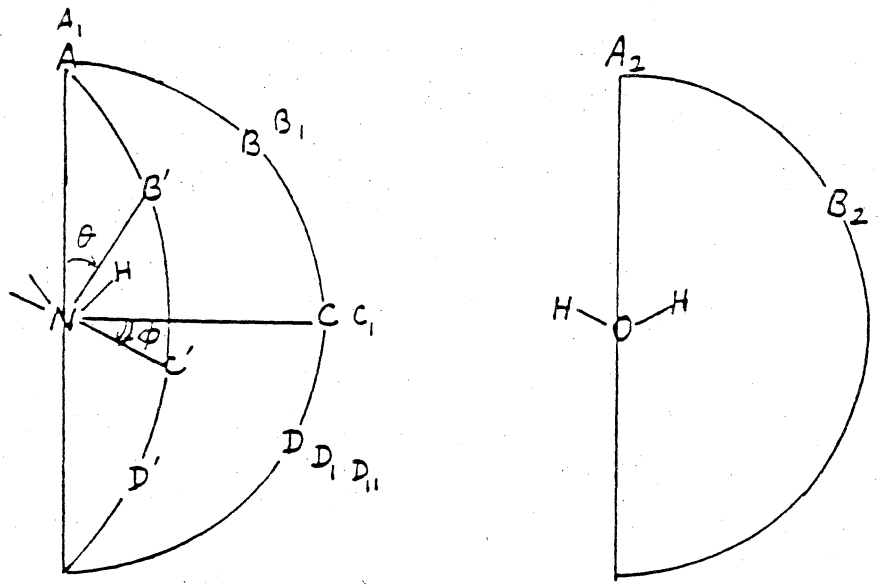

Fig. 1 Configurations of $(NH_3)_2$ and $NH_3 \cdot H_2O$ adopted in optimization of empirical parameters.

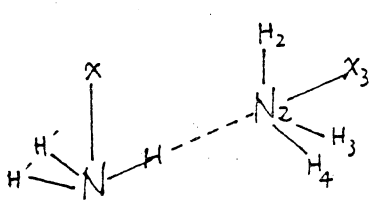

X_3 along the line of NN_2; dihedral angle of XNN_2H_2 =0 Deg.

B -linear

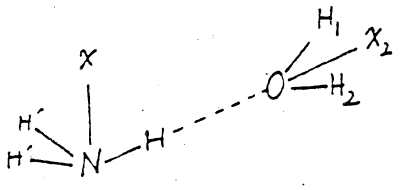

X_2 along the line of NO; plane NH_1H_2 ⊥ plane XNO

B_1 -linear

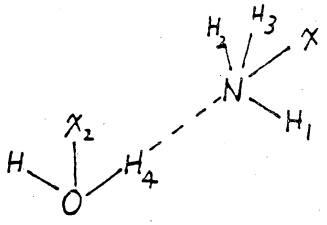

X along the line of ON; dihedral angle of $HONH_1$ =180 deg.

B_2 -linear

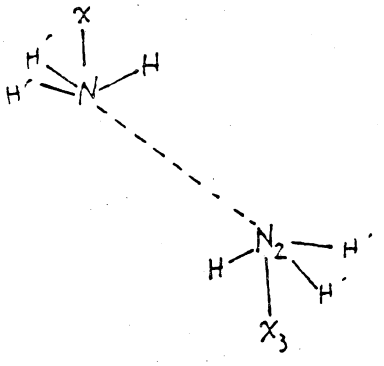

$X//X_3$; $\angle XNN_2 = \angle NN_2X_3$ =128.47 deg.

D-cyclic

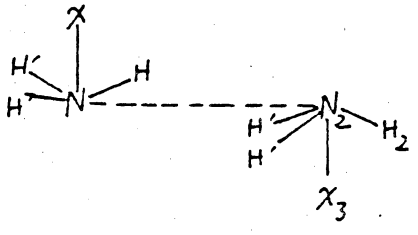

$X//X_3$; dihedral angle HNN_2H_2 = 180 deg.

C type

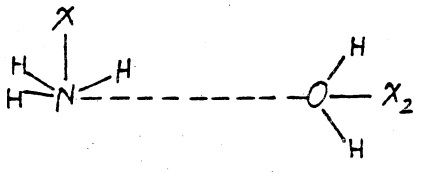

$X \perp NO$; X_2 along the line of NO

C_1 type

Fig. 2 $(NH_3)_2$ and $NH_3 \cdot H_2O$ Dimer Configurations by Type.

X =3 fold axis of an ammonia monomer;
X_3=3 fold axis of the 2nd ammonia monomer;
X_2=2 fold axis of a water monomer;
The orientation of the 2nd monomer in B', C' or D' is turned an angle ϕ around XN.

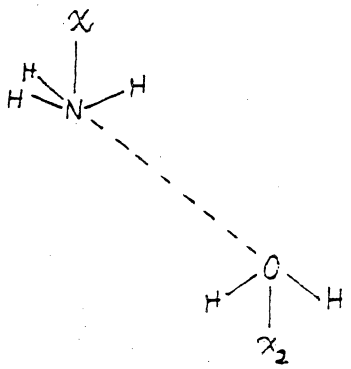

$X//X_2$;
$\angle XNO = \angle X_2ON$
$=128.47$ deg.
D_1-cyclic

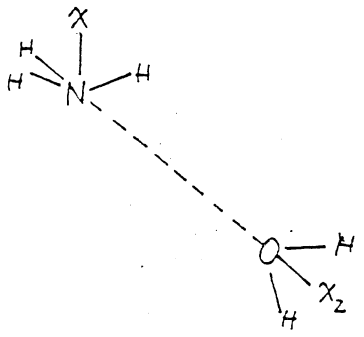

X_2 along the line of NO; $\angle XNO =$ 128.47 deg.
D_{11}-cyclic

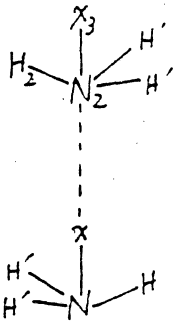

X along the line of X_3; dihedral angle $HNN_2H_2=180$ deg.
A-bifurcated

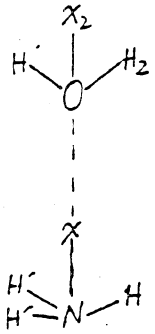

X along the line of X_2; dihedral angle $HNOH_2 = 0$ deg.
A_1-bifurcated

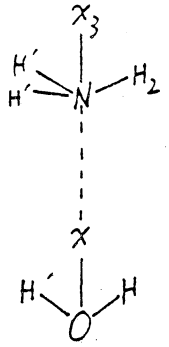

X along the line of X_3; dihedral angle $HONH_2 = 0$ deg.
A_2-bifurcated

Fig. 2 $(NH_3)_2$ and $NH_3 \cdot H_2O$ Dimer Configurations by Type. (continued)
X =3 fold axis of an ammonia monomer;
X_3=3 fold axis of the 2nd ammonia monomer;
X_2=2 fold axis of a water monomer;
The orientation of the 2nd monomer in B', C' or D' is turned an angle ϕ around XN.

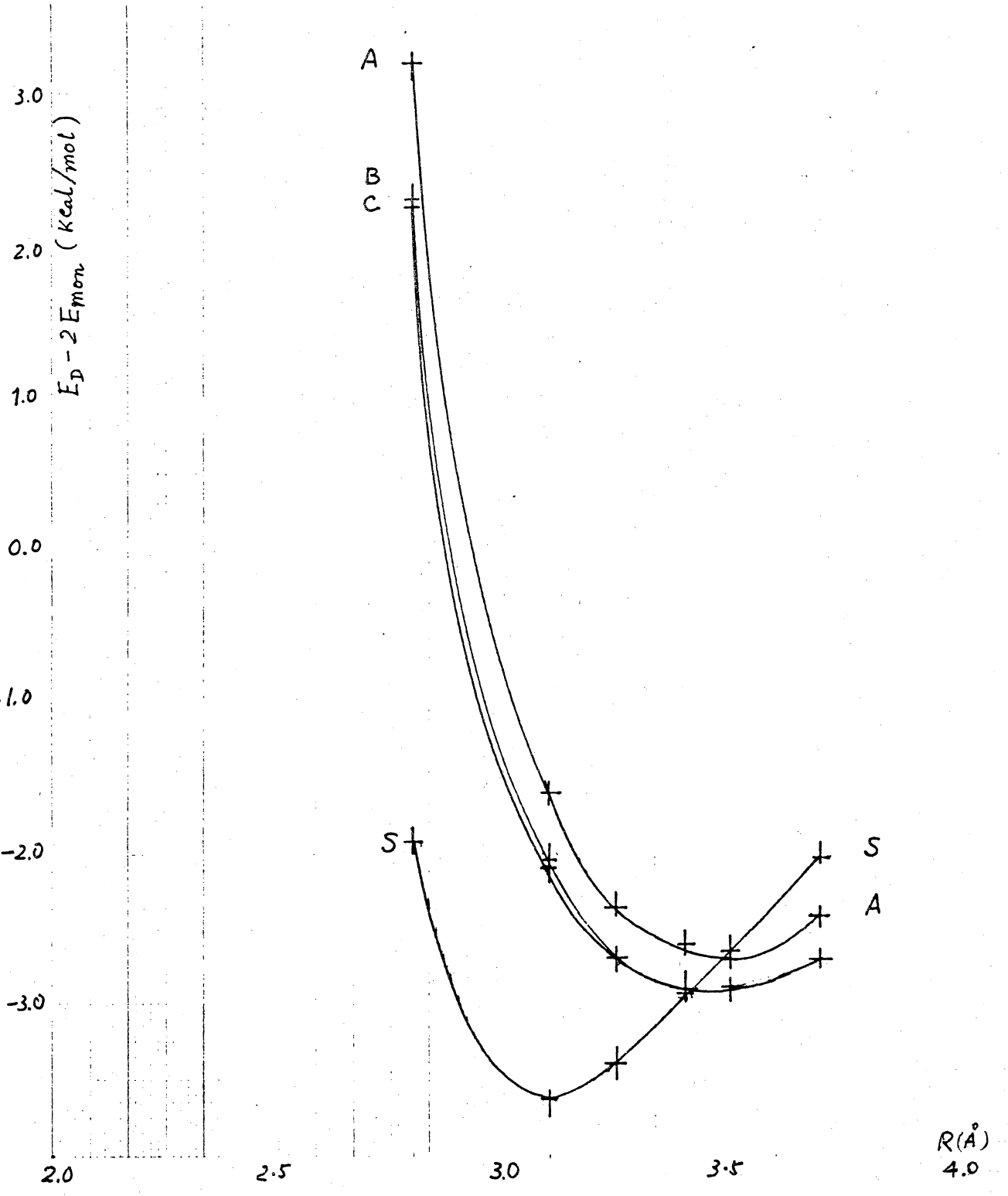

Figure 3. Comparison of the curves calculated with different basis sets for the linear dimers of ammonia
A - Kollman and Allen [10b] B - 6-31G**
C - 6-31G* S - STO-3G

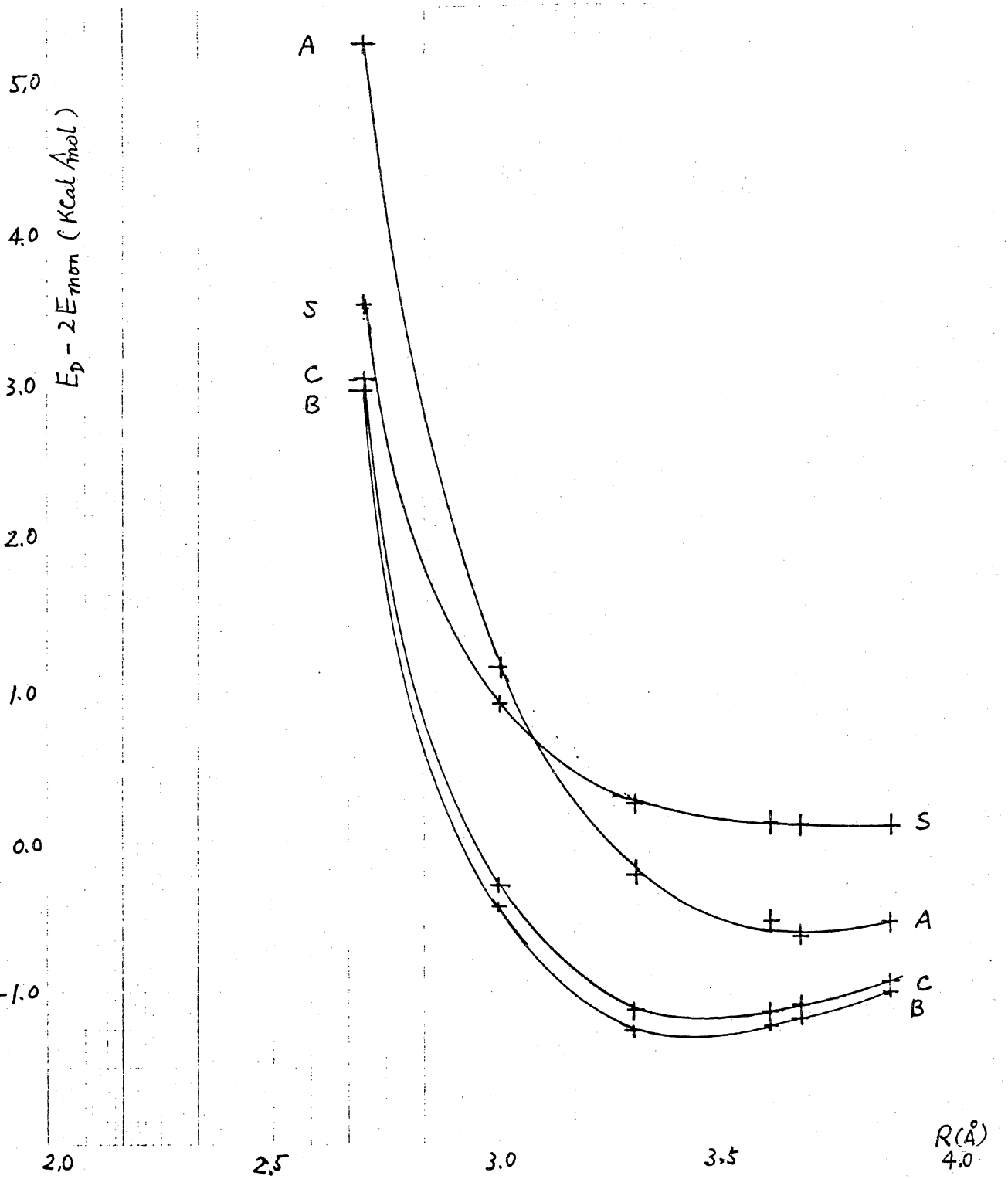

Figure 4. Comparison of the curves calculated with different basis sets for the cyclic dimers of ammonia

A - Kollman and Allen[10b] B - 6-31G**

C - 6-31G* S - STO-3G

Description of the Empirical Potential

1. Pairwise

The total H-bonding energy for a water oligomer composed of n monomers can be defined as: $E_H = E_T - n \bullet E^{(1)}$, where E_T is the total energy and $E^{(1)}$ is the energy of the monomer.

The total H-bonding energy can be considered to be composed of pairwise energies and higher order interaction terms which are referred to as non-additive terms. The pairwise energy is the sum of the interaction energies between all possible pairs of monomers in the absence of other interacting molecules. Non-additive energies can be estimated through the following relationships:[27]

$$V^{(2)} = E_T^{(2)} - 2 \bullet E^{(1)}.$$

$$V^{(3)} = E_T^{(3)} - 3 \bullet E^{(1)} - \Sigma V^{(2)}.$$

$$V^{(n)} = E_T^{(n)} - n \bullet E^{(1)} - \Sigma V^{(2)} - \Sigma V^{(3)} - \bullet\bullet - V^{(n-1)}$$

where $E_T^{(n)}$ is the total energy of n bodies and $E^{(1)}$ is the energy of the monomer. In the case of a dimer the H-bonding energy is exactly equal to the pairwise dimerization energy: $E_H = V^{(2)} = E_T^{(2)} - 2E^{(1)}$. For an oligomer with n larger than 2, non-additive energies must also be included.

2. *Parameters*

Our empirical potential for the interaction between a pair of monomers is composed of van der Waals interactions and electrostatic contributions.

$$E_H = \Sigma E_{VDW} + \Sigma q_i \bullet q_j / r_{ij}$$

Van der Waals interactions between all pairs of atoms in different molecules are computed using the Hill equations (1) and (1a) with parameters for O, N and H taken from Allinger's MM2 program.[18b] Although Allinger uses van der Waals interactions involving lone pair pseudoatoms, these are not included in our intermolecular potential.

$$E_{VDW} = \varepsilon(2.9 \times 10^5 \exp(-12.5/P) - 2.25P^6), \qquad \text{if } P < 3.311 \text{ (1)}$$

$$E_{VDW} = \varepsilon \times 336.176P^2, \qquad \text{if } P > 3.311 \text{ (1a)}$$

where $P = r^*/R$

R = effective internuclear distance

r^* = summation of the VDW radii of the two atoms involved, in A

ε = geometrical average of the "hardness" of the two atoms, in kcal/mol

r^* and ε can be calculated based on Allinger's table.[16]

To describe the coulombic interactions, partial positive charges were placed in the line of each X-H bond (X = O,N), and negative charges in the line of each X-Lp bond (Lp = lone pair) as shown in Figure 5. The locations of the lone pairs are the same as defined by Taylor.[3] The charges were constrained so that the total charge on any monomer is zero.

The optimized parameters (shown in Figure 4) are |q| = 0.226 a.u., RHp = -0.584 A, ROn = 0.0349 A for H_2O and |q| = 0.312 a.u., RHp = -0.239 A, RNn = -0.178 A for NH_3. RHp is the distance from H to the positive charge along the O-H line or N-H line; the minus sign means

that the charge lies outside the O-H bond or N-H bond. ROn is the distance between O and the negative charge along the line from O to the center of a lone pair. Equivalent meanings are used for the remaining parameters.

3. Root Mean Square Deviation

The RMS deviation of the 216 configurations is 0.9 kcal/mol, where the ab initio results of Matsuoka and those of 6-31G* are adopted as standards. The RMS deviation using Taylor potential is 1.42 kcal/mol and that of Kroon's is 0.6 kcal/mol for the 66 configurations of water dimers. Our parameters were optimized based on 216 configurations of water dimers, ammonia dimers and mixed dimers. Using these parameters, the RMS deviation of the ab initio versus empirical interaction energies from our potential is 0.87 kcal/mol for 61 configurations of the water dimers.

In a separate optimization, the resulted parameters of CH_3OH monomer are also listed in Fig. 5. The RMS deviation is 0.5 kcal/mol for 61 configurations of methanol dimers.

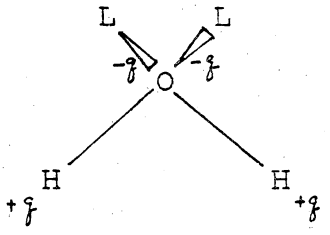

L - lone pair electrons

|q| = 0.226 a.u.

RHp =-0.584 A

ROn = 0.0349 A

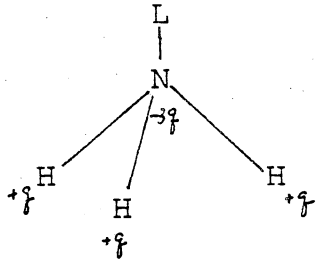

|q| = 0.312 a.u.

RHp =-0.239 A

RNn =-0.178 A

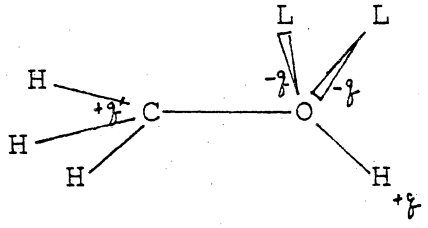

L - lone pair electrons

|q| = 0.20 a.u.

|q'| = 0.20 a.u.

ROn = 0.076 A

RHp =-0.58 A

RCp =-0.72 A

Fig. 5 Point charge models

Table 1 Comparison of dimerization energies of $(H_2O)_2$ calculated *(in kcal/mol)*

Geometrical types A-I are shown in References 13 and 3a.

Emp. = Empirical potential, this work
MCY = Ab initio results by MCY
Tay = Taylor's empirical results
Kroon = Kroon-Batenburg & Kanterss' results
6-31G*= Ab initio 6-31G* basis, this work

d(OO) A	2.38	2.65	2.91	3.18	3.70	4.23	4.76	5.82	7.94
A type									
MCY	2.10	-3.64	-5.14	-4.17	-3.11	-2.00	-1.24	-0.53	-0.15
Tay	7.30	-1.88	-4.06	-3.67	-2.16	-1.22	-0.73	-0.33	-0.11
Kroon	1.13	-4.28	-5.20	-4.38	-2.59	-1.51	-0.94	-0.42	-0.14
Emp	1.17	-3.62	-5.03	-4.49	-2.72	-1.61	-1.01	-0.47	-0.16
Emp-MCY	-0.93	0.02	0.11	0.22	0.39	0.39	0.23	0.06	-0.01
Emp-Kroon	0.04	0.66	0.17	-0.11	-0.13	-0.10	-0.07	-0.05	-0.02
Emp-Tay	-6.13	-1.74	-0.97	-0.82	-0.56	-0.39	-0.28	-0.14	-0.05
B type									
MCY	4.72	-2.08	-3.98	-4.09	-3.01	-2.15	-1.54	-0.64	-0.18
Tay	2.19	-3.62	-4.00	-3.37	-2.15	-1.41	-0.97	-0.52	-0.20
Kroon	5.32	-2.72	-4.46	-4.33	-2.99	-1.94	-1.30	-0.66	-0.25
Emp	1.62	-1.96	-2.75	-2.64	-1.95	-1.38	-1.01	-0.58	-0.24
Emp-MCY	-3.10	0.12	1.23	1.45	1.06	0.77	0.53	0.06	-0.06
Emp-Kroon	-3.70	0.76	1.71	1.69	1.04	0.56	0.29	0.08	0.01
Emp-Tay	-0.57	1.66	1.25	0.73	0.20	0.03	-0.04	-0.06	-0.04
C type									
MCY	1.08	-4.02	-4.89	-4.21	-2.90	-1.79	-1.22	-0.41	-0.15
Tay	3.61	-3.11	-3.63	-2.99	-1.75	-1.05	-0.67	-0.32	-0.11
Kroon	1.56	-3.97	-4.55	-3.86	-2.31	-1.34	-0.84	-0.39	-0.13
Emp	1.04	-3.43	-4.02	-3.51	-2.23	-1.41	-0.93	-0.46	-0.16
Emp-MCY	-0.04	0.59	0.87	0.70	0.67	0.38	0.29	-0.05	-0.01
Emp-Kroon	-0.52	0.54	0.53	0.35	0.08	-0.07	-0.09	-0.07	-0.03
Emp-Tay	-2.57	-0.32	-0.39	-0.52	-0.48	-0.36	-0.26	-0.14	-0.05
D type									
MCY	4.72	-3.16	-5.40	-5.21	-3.57	-2.44	-1.67	-0.65	-0.18
Tay	2.19	-3.15	-5.16	-4.44	-2.70	-1.60	-1.01	-0.50	-0.20
Kroon	5.21	-4.83	-5.42	-4.43	-2.76	-1.74	-1.16	-0.61	-0.25
Emp	1.62	-3.52	-5.86	-5.08	-3.11	-1.91	-1.24	-0.62	-0.24
Emp-MCY	-3.10	-0.36	-0.46	0.13	0.46	0.53	0.43	0.03	-0.06
Emp-Kroon	-3.59	1.31	-0.44	-0.65	-0.35	-0.17	-0.08	-0.01	0.01
Emp-Tay	-0.57	-0.37	-0.70	-0.64	-0.41	-0.31	-0.23	-0.12	-0.04

Table 1 Comparison of dimerization energies of $(H_2O)_2$ calculated (continued)

E type					
MCY	5.67	-3.58	-5.55	-5.32	-3.65
Tay	5.32	-3.94	-5.20	-4.54	-2.76
Kroon	7.14	-5.62	-5.81	-4.73	-2.90
Emp	4.89	-4.35	-5.73	-5.03	-3.13
Emp-MCY	-0.78	-0.77	-0.18	0.29	0.52
Emp-Kroon	-2.25	1.27	0.08	-0.30	-0.23
Emp-Tay	-0.43	-0.41	-0.53	-0.49	-0.37
F type					
MCY	0.55	-3.81	-4.99	-4.40	-3.14
Tay	1.68	-3.15	-4.31	-3.85	-2.37
Kroon	1.41	-3.42	-4.41	-3.91	-2.47
Emp	2.05	-2.99	-4.76	-4.51	-2.91
Emp-MCY	1.50	0.82	0.23	-0.11	0.23
Emp-Kroon	0.64	0.43	-0.35	-0.60	-0.44
Emp-Tay	0.37	0.16	-0.45	-0.66	-0.54
G type					
MCY	3.38	-2.55	-3.91	-3.73	-2.97
Tay	1.40	-3.54	-3.73	-3.09	-1.93
Kroon	3.54	-3.08	-4.28	-3.96	-2.65
Emp	0.87	-2.96	-3.43	-3.02	-2.00
Emp-MCY	-2.51	-0.41	0.48	0.71	0.97
Emp-Kroon	-2.67	0.12	0.85	0.94	0.65
Emp-Tay	-0.53	0.58	0.30	0.07	-0.07
H type					
MCY	2.62	-3.61	-4.88	-4.33	-3.03
Tay	5.85	-2.76	-3.77	-3.21	-1.91
Kroon	1.95	-4.35	-4.92	-4.16	-2.50
Emp	1.64	-3.59	-4.26	-3.70	-2.33
Emp-MCY	-0.98	0.02	0.62	0.63	0.70
Emp-Kroon	-0.31	0.76	0.66	0.46	0.17
Emp-Tay	-4.21	-0.83	-0.49	-0.49	-0.42
I type					
MCY	-0.05	-4.22	-4.89	-4.31	-3.01
Tay	0.57	-3.35	-3.86	-3.27	-1.94
Kroon	0.00	-4.09	-4.59	-3.94	-2.42
Emp	0.67	-3.28	-4.27	-3.91	-2.52
Emp-MCY	0.72	0.94	0.62	0.40	0.49
Emp-Kroon	0.67	0.81	0.32	0.03	-0.10
Emp-Tay	0.10	0.07	-0.41	-0.64	-0.58

Table 2 Comparison of dimerization energies of $(NH_3)_2$ calculated (in kcal/mol)

θ and φ in degree. d in Angstrom.

A type - bifurcated

d(NN)	2.7	3.0	3.3	3.6	3.9	4.2	4.4	4.6	4.8	5.0
θ	0.	0.	0.	0.	0.	0.	0.	0.	0.	0.
φ	-	-	-	-	-	-	-	-	-	-
6-31G*	7.43	1.85	-0.31	-1.01	-1.08	-0.94	-0.83	-0.74	-0.66	-0.59
Emp	2.52	0.62	0.00	-0.18	-0.22	-0.22	-0.21	-0.20	-0.19	-0.18
Dif	-4.91	-1.23	0.31	0.83	0.86	0.72	0.62	0.54	0.47	0.41

B type - linear

d(NN)	2.8	3.1	3.3	3.4	3.5	3.7
θ	68.3	68.3	68.3	68.3	68.3	68.3
φ	0.0	0.0	0.0	0.0	0.0	0.0
6-31G*	2.25	-2.08	-2.70	-2.89	-2.88	-2.71
Emp	1.52	-2.01	-2.33	-2.29	-2.18	-1.85
Dif	-0.73	0.07	0.37	0.60	0.70	0.86

d(NN)	4.0	4.2	4.4	4.6	4.8	5.0
θ	68.3	68.3	68.3	68.3	68.3	68.3
φ	0.0	0.0	0.0	0.0	0.0	0.0
6-31G*	-2.30	-1.98	-1.65	-1.34	-1.07	-0.86
Emp	-1.39	-1.13	-0.93	-0.76	-0.63	-0.53
Dif	0.91	0.85	0.72	0.58	0.44	0.33

B' type

d(NN)	2.8	3.1	3.3	3.4	3.5	3.7	2.8	3.1	3.3	3.4
θ	68.3	68.3	68.3	68.3	68.3	68.3	68.3	68.3	68.3	68.3
φ	30.	30.	30.	30.	30.	30.	60.	60.	60.	60.
6-31G*	2.89	-1.01	-1.69	-1.98	-2.04	-2.00	2.94	-0.30	-0.95	-1.27
Emp	0.89	-1.22	-1.43	-1.42	-1.37	-1.19	0.82	-0.41	-0.58	-0.63
Dif	-2.00	-0.21	0.26	0.56	0.67	0.81	-2.12	-0.11	0.37	0.64

d(NN)	3.5	3.7	2.8	3.1	3.3	3.4	3.5	3.7
θ	68.3	68.3	68.3	68.3	68.3	68.3	68.3	68.3
φ	60.	60.	90.	90.	90.	90.	90.	90.
6-31G*	-1.36	-1.39	2.89	-1.01	-1.69	-1.98	-2.04	-2.00
Emp	-0.63	-0.58	0.89	-1.22	-1.43	-1.42	-1.37	-1.19
Dif	0.73	0.81	-2.00	-0.21	0.26	0.56	0.67	0.81

C type

d(NN)	2.7	3.0	3.3	3.6	3.9
θ	90.	90.	90.	90.	90.
φ	0.	0.	0.	0.	0.
6-31G*	7.56	0.82	-1.04	-1.29	-1.11
Emp	6.23	-0.62	-1.87	-1.67	-1.25
Dif	-1.33	-1.44	-0.83	-0.38	-0.14

Table 2 Comparison of dimerization energies of $(NH_3)_2$ calculated (continued)

θ and φ in degree. d in Angstrom.

C' type

d(NN)	2.7	3.0	3.3	3.6	3.9	2.7	3.0	3.3	3.6	3.9
θ	90.	90.	90.	90.	90.	90.	90.	90.	90.	90.
φ	30.	30.	30.	30.	30.	60.	60.	60.	60.	60.
6-31G*	5.91	0.50	-0.95	-1.14	-0.99	4.07	0.06	-0.94	-1.03	-0.89
Emp	5.55	0.08	-1.08	-1.09	-0.86	3.87	0.30	-0.56	-0.65	-0.56
Dif	-0.36	-0.42	-0.13	0.05	0.13	-0.20	0.24	0.38	0.38	0.33

d(NN)	2.7	3.0	3.3	3.6	3.9
θ	90.	90.	90.	90.	90.
φ	90.	90.	90.	90.	90.
6-31G*	5.91	0.50	-0.95	-1.14	-0.99
Emp	5.55	0.08	-1.08	-1.09	-0.86
Dif	-0.36	-0.42	-0.13	0.05	0.13

D type - cyclic

d(NN)	2.7	3.0	3.3	3.6	3.9	4.2	4.4	4.6	4.8	5.0
θ	128.5	128.5	128.5	128.5	128.5	128.5	128.5	128.5	128.5	128.5
φ	0.	0.	0.	0.	0.	0.	0.	0.	0.	0.
6-31G*	3.05	-0.27	-1.13	-1.14	-0.90	-0.63	-0.49	-0.38	-0.29	-0.23
Emp	0.57	-0.70	-0.86	-0.73	-0.57	-0.42	-0.35	-0.29	-0.24	-0.20
Dif	-2.48	-0.43	0.27	0.41	0.33	0.21	0.14	0.09	0.05	0.03

D' type

d(NN)	2.7	3.0	3.3	3.6	3.9	2.7	3.0	3.3	3.6	3.9
θ	128.5	128.5	128.5	128.5	128.5	128.5	128.5	128.5	128.5	128.5
φ	30.	30.	30.	30.	30.	60.	60.	60.	60.	60.
6-31G*	2.86	-0.15	-0.94	-0.96	-0.75	2.63	-0.06	-0.76	-0.79	-0.62
Emp	0.85	-0.40	-0.62	-0.55	-0.43	1.15	-0.10	-0.37	-0.37	-0.29
Dif	-2.01	-0.25	0.32	0.41	0.32	-1.48	-0.04	0.39	0.42	0.33

d(NN)	2.7	3.0	3.3	3.6	3.9
θ	128.5	128.5	128.5	128.5	128.5
φ	90.	90.	90.	90.	90.
6-31G*	2.86	-0.15	-0.94	-0.96	-0.75
Emp	0.85	-0.40	-0.62	-0.55	-0.43
Dif	-2.01	-0.25	0.32	0.41	0.32

Table 3 Comparison of dimerization energies of ($H_2O \cdot NH_3$) calculated (*in kcal/mol*)

θ and φ in degree. d in Angstrom.

A1 type - bifurcated, 3H from ammonia monomer

d(NO)	2.7	3.0	3.3	3.6	3.9	4.2	4.4	4.6	4.8	5.0
θ	0.	0.	0.	0.	0.	0.	0.	0.	0.	0.
φ	0.	0.	0.	0.	0.	0.	0.	0.	0.	0.
6-31G*	3.19	0.06	-0.93	-1.07	-0.95	-0.79	-0.71	-0.64	-0.58	-0.53
Emp	1.88	0.42	-0.06	-0.21	-0.25	-0.25	-0.24	-0.23	-0.22	-0.21
Dif	-1.31	0.36	0.87	0.86	0.70	0.54	0.47	0.41	0.36	0.32

A2 type - bifurcated, 2H from water monomer

d(ON)	2.7	3.0	3.3	3.6	3.9	4.2	4.4	4.6	4.8	5.0
θ	0.	0.	0.	0.	0.	0.	0.	0.	0.	0.
φ	0.	0.	0.	0.	0.	0.	0.	0.	0.	0.
6-31G*	0.14	-3.35	-3.96	-3.59	-2.97	-2.34	-1.98	-1.68	-1.44	-1.25
Emp	-1.19	-2.23	-2.15	-1.82	-1.49	-1.22	-1.07	-0.94	-0.83	-0.73
Dif	-1.33	1.12	1.81	1.77	1.48	1.12	0.91	0.74	0.61	0.52

B1 type - linear, H from ammonia monomer

d(NO)	2.7	3.0	3.3	3.6	3.9	4.2	4.4	4.6	4.8	5.0
θ	68.3	68.3	68.3	68.3	68.3	68.3	68.3	68.3	68.3	68.3
φ	0.	0.	0.	0.	0.	0.	0.	0.	0.	0.
6-31G*	3.44	-1.30	-2.22	-2.11	-1.76	-1.35	-1.10	-0.89	-0.73	-0.60
Emp	3.13	-1.51	-2.12	-1.80	-1.38	-1.04	-0.86	-0.72	-0.60	-0.51
Dif	-0.31	-0.21	0.10	0.31	0.38	0.31	0.24	0.17	0.13	0.09

B2 type - linear, H from water monomer

d(ON)	2.7	3.0	3.3	3.6	3.9	4.2	4.4	4.6	4.8	5.0
θ	52.8	52.8	52.8	52.8	52.8	52.8	52.8	52.8	52.8	52.8
φ	0.	0.	0.	0.	0.	0.	0.	0.	0.	0.
6-31G*	-3.86	-6.35	-5.87	-4.82	-3.81	-2.92	-2.40	-1.95	-1.59	-1.31
Emp	-5.18	-6.03	-4.85	-3.59	-2.62	-1.94	-1.60	-1.33	-1.12	-0.95
Dif	-1.32	0.32	1.02	1.23	1.19	0.98	0.80	0.62	0.47	0.36

C1 type

d(NO)	2.7	3.0	3.3	3.6	3.9	4.2	4.4	4.6	4.8	5.0
θ	90.	90.	90.	90.	90.	90.	90.	90.	90.	90.
φ	0.	0.	0.	0.	0.	0.	0.	0.	0.	0.
6-31G*	3.49	-0.35	-1.21	-1.23	-1.02	-0.76	-0.59	-0.46	-0.35	-0.28
Emp	2.20	-0.96	-1.40	-1.19	-0.90	-0.66	-0.54	-0.44	-0.37	-0.31
Dif	-1.29	-0.61	-0.19	0.04	0.12	0.10	0.05	0.02	-0.02	-0.03

D11 type

d(NO)	2.7	3.0	3.3	3.6	3.9	4.2	4.4	4.6	4.8	5.0
θ	128.5	128.5	128.5	128.5	128.5	128.5	128.5	128.5	128.5	128.5
φ	0.	0.	0.	0.	0.	0.	0.	0.	0.	0.
6-31G*	6.47	3.33	1.99	1.40	1.12	0.93	0.83	0.74	0.66	0.59
Emp	2.75	1.49	0.98	0.73	0.59	0.49	0.43	0.39	0.35	0.31
Dif	-3.72	-1.84	-1.01	-0.67	-0.53	-0.44	-0.40	-0.35	-0.31	-0.28

Table 3 Comparison of dimerization energies of ($H_2O \cdot NH_3$) calculated (continued)

θ and ϕ in degree. d in Angstrom.

D1 type - cyclic

d(NO)	2.7	3.0	3.3	3.6	3.9	4.2	4.4	4.6	4.8	5.0
θ	128.5	128.5	128.5	128.5	128.5	128.5	128.5	128.5	128.5	128.5
ϕ	0.	0.	0.	0.	0.	0.	0.	0.	0.	0.
6-31G*	0.15	-1.20	-1.30	-1.04	-0.74	-0.51	-0.41	-0.33	-0.27	-0.22
Emp	0.55	-0.32	-0.47	-0.42	-0.34	-0.27	-0.23	-0.19	-0.16	-0.14
Dif	0.40	0.88	0.83	0.62	0.40	0.24	0.18	0.14	0.11	0.08

Applications

Dimers: $(H_2O)_2$, $(NH_3)_2$, $NH_3 \bullet H_2O$ and $(CH_3OH)_2$

$(H_2O)_2$

The geometrical parameters of the water dimer as determined from a supersonic nozzle beam experiment are d(O-O) = 2.98 ± 0.01 A; α = 58 ± 6 degree.[28]

Using the experimental structure discussed above along with the empirical potential described previously, the calculated dimerization energy for $(H_2O)_2$ is -5.74 kcal/mol. This is based on d(O-H) = 0.9572 A, HOH = 104.52 degree, d(O-O) = 2.981 A and α = 58.6 degree (the acute angle between O-O line and H-O-H plane, see Fig. 6).

An accurate determination of the experimental dimerization energy of $(H_2O)_2$ is difficult due to the small percentage of dimers in the gas phase. However, a number of experimental results have been reported. In 1979 a dimerization enthalphy of ΔH = -3.59 kcal/mol at 373K was determined

from a thermal conductivity experiment. The dimerization energy was estimated to have the value -5.44 ± 0.70 kcal/mol[29] when corrected for thermal and zero point contributions. The ΔE from an ab initio or empirical calculation is equivalent to ΔE(elec.), the energy difference between two electronic states with zero vibrational energies. The relationship between ΔH and ΔE(elec.), as shown in Ref. 29, is:

$$\Delta E(\text{elec.}) + \Delta E(\text{vib.}) + \Delta E(\text{rot.}) + \Delta E(\text{trans.}) = \Delta H - \Delta(PV).$$

where the summation of the left hand side is equal to ΔE(thermodynamic).

An association enthalpy for the water dimer of -5.2 ± 1.5 kcal/mol (ΔE = -7.1 ± 1.5 kcal/mol after a correction of -1.85 kcal/mol[26]) has also been determined from the variation of infrared absorption intensity with temperature[30]. Analysis of second virial coefficient data[31,32] have given ΔH values ranging between -3.3 and -4.5 kcal/mol (ΔE = -5.15 to -6.35 kcal/mol after the -1.85 kcal/mol correction[29]). Based on Popkies' Hartree Fock limit for the dimerization energy and MCYs' electronic correlation effect, Curtiss et al. estimated the theoretical ab initio dimerization energy of $(H_2O)_2$ to be -5.0 ± 0.45 Kcal/mol.[29] A comparison of the calculated and experimental values is given in Table 4.

$(NH_3)_2$

Experimental values of dimerization enthalpies for $(NH_3)_2$ range from -3.6 kcal/mol to -4.61 kcal/mol.[33-36] After the classical correction of -2RT, -1.18 kcal/mol at 298K, the range is from -4.78 to -5.79 kcal/mol for ΔE. The experimental results are apparently subject to question.[37] The empirical value based on our potential was -2.3 kcal/mol for the linear ammonia dimer with d(N-N) = 3.4 A (Table 4). Ab initio results for the dimerization energy of ammonia varies with the basis set used. They have been reported in a range of -2.7 to -4.5 kcal/mol.[37] (see Table 1 in Ref. 37.) A linear dimer with d(N-N) = 3.4 A had a dimerization energy of -2.9 kcal/mol[37] when a

α = 58.± 6° [a]

d(O-O)= 2.98±0.01 A

d(O-H)= 0.96 A

∠HOH= 104.52°

a -Reference 28

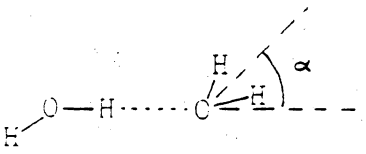

Fig. 6 Geometry of water dimer

Table 4 Comparison of Experimental and Calculated Dimerization Energies

Water dimer Method	kcal/mol	Remarks
6-31G*	-5.2	Ref. 24
6-31G*	-5.6	$\alpha=55°$, Ref. 37
Thermal conductivity	-5.4+0.7	Ref. 29
IR	-7.1+1.5	ΔE, Ref. 30
2nd virial coefficient	-5.15 to -6.35	ΔE, Ref. 29
Taylor potential	-5.35	Ref. 3a
This work	-5.74	$\alpha=58.6°$

Ammonia dimer Method	kcal/mol	Remarks
6-31G*	-2.9	d(NN)=3.4 A, Ref. 37
STO-3G	-3.74	d(NN)=3.067A, Ref. 12a
Experiments	-4.78 to -5.79	ΔE, Ref. 33-36
This work	-2.3	d(NN)=3.44 A, linear

6-31G* basis was used. Using a STO-3G basis set, Jorgensen et al. obtained -3.74 kcal/mol for a slightly bent hydrogen bond with d(N-N) = 3.067 A.[12a]

Semiempirical and empirical results reported are -3.2 kcal/mol for a constrained linear ammonia dimer, -2.47 kcal/mol for an eclipsed near-linear dimer, -2.45 kcal/mol for a staggered linear dimer and -2.27 kcal/mol for a closed cyclic dimer.[38]

Mixed Dimers

Dill et al.[37] have also calculated ab initio results for $NH_3 \bullet H_2O$ and $H_2O \bullet NH_3$. Some of their results are listed in Table 5 for comparison. Although the geometries used are not exactly the same, our energies compare favorably to those calculated by Kollman[10b] and Dill.

Methanol Dimers

Following the same procedure as was used for the water, ammonia and mixed dimers, we optimized the charges and their locations in a methanol monomer (Fig. 5) by fitting the empirical dimerization energies of the sixty one mathanol dimers to the dimerization energies calculated using 6-31G* basis sets. Comparisons between the empirical dimerization energies and those energies computed by ab initio method are shown in Table 6. Differences larger than 1.1 kcal/mol occur in the repulsive configurations.

Table 5 Comparisons of Dimerization Energies of $(NH_3)_2$ and $NH_3 \cdot H_2O$. (in kcal/mol)

	d(NH)	HNH	d(OH)	HOH	Remarks
a	1.0116	106.7	0.957	105.	Kollman et al.[10b]
b	1.0136	107.05	0.957	104.52	Dill et al.[37]
c	1.0025	107.2	0.9473	105.5	This work

Units are in A or degree.

$H_3N...H-NH_2$					Remarks
d(NN) A	3.4	3.44	3.49	3.5	
α	0.	0.	0.	0.	
HFAO			-2.7		a
6-31G*		-2.9			b
6-31G*	-2.89			-2.88	c
EMP	-2.29			-2.18	c

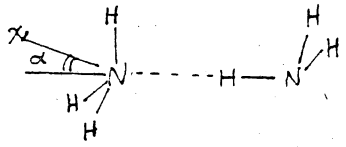

$H_3N...H-OH$					Remarks
d(NO) A	3.0	3.05	3.12	3.3	
α	0.	0.	0.	0.	
HFAO			-5.8		a
6-31G*		-6.5			b
6-31G*	-6.35			-5.87	c
EMP	-6.03			-4.85	c

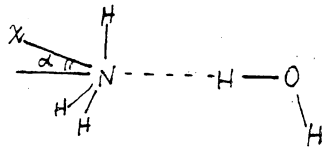

$H_2O...H-NH_2$					Remarks
d(ON) A	3.3	3.40[1]	3.40	3.41	
α	0.	68.7	68.7	0.	
HFAO				-2.3	a
6-31G*		-2.8			b
6-31G*	-2.22				c
emp	-2.12	-2.12	-2.07		c

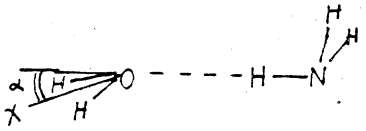

1. Monomer geometry is the same as Dills'.

Table 6 Comparisons of dimerization energies of methanol dimers from empirical and ab initio calculations (in kcal/mol)

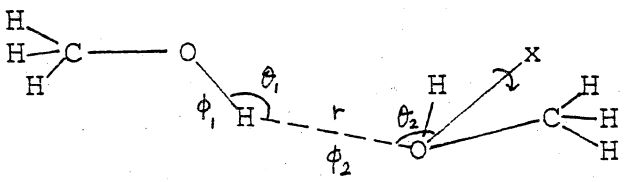

Emp.	6-31G*	Dif.	r	θ_1	θ_2	ϕ_1	ϕ_2	χ
5.41	4.79	0.62	1.50	163.	132.	180.	180.	90.
-3.59	-3.46	-0.13	1.94	"	"	"	"	"
-3.68	-3.59	-0.09	1.99	"	"	"	"	"
-2.70	-2.83	0.13	2.50	"	"	"	"	"
-4.77	-4.90	0.13	1.94	"	"	"	0.	"
-0.57	-0.80	0.23	1.94	120.	"	"	"	"
-3.90	-4.34	0.44	1.94	150.	"	"	"	"
-5.18	-5.09	-0.09	1.94	180.	"	/	"	"
-5.20	-5.15	-0.05	1.99	"	"	/	"	"
-4.82	-4.98	0.16	1.99	163.	"	180.	"	"
-3.95	-3.11	-0.84	1.94	150.	"	0.	"	"
12.16	10.44	1.72	1.94	163.	60.	180.	"	"
-4.25	-3.65	-0.60	"	"	90.	"	"	"
-4.88	-4.99	0.11	"	"	120.	"	"	"
-4.58	-4.63	0.05	"	"	150.	"	"	"
-4.28	-4.26	-0.02	"	"	175.	"	"	"
13.07	13.56	-0.49	1.70	120.	90.	"	"	"
4.20	4.85	-0.65	"	"	120.	"	"	"
4.72	6.14	-1.42	"	"	150.	"	"	"
1.07	0.65	0.42	"	150.	90.	"	"	"
-1.46	-2.10	0.64	"	"	120.	"	"	"
-1.02	-1.33	0.31	"	"	150.	"	"	"
-1.43	-0.39	-1.04	"	180.	90.	/	"	"
-3.35	-3.08	-0.27	"	"	120.	/	"	"
-3.49	-3.19	-0.30	"	"	150.	/	"	"
1.32	0.85	0.47	1.99	120.	90.	180.	"	"
-1.33	-1.94	0.61	"	"	120.	"	"	"
-0.45	-0.53	0.08	"	"	150.	"	"	"
-3.73	-3.68	-0.05	"	150.	90.	"	"	"
-4.23	-4.72	0.49	"	"	120.	"	"	"
-3.71	-4.06	0.35	"	"	150.	"	"	"
-4.59	-3.53	-1.06	"	180.	90.	/	"	"
-5.20	-5.07	-0.13	"	"	120.	/	"	"
-5.16	-5.08	-0.08	"	"	150.	/	"	"

r in Å, angles in degree

Table 6 Comparisons of dimerization energies of methanol dimers from empirical and ab initio calculations (continued)

Emp.	6-31G*	Dif.	r	θ_1	θ_2	ϕ_1	ϕ_2	χ
-2.60	-3.16	0.56	2.50	120.	90.	180.	0.	90.
-2.14	-2.90	0.76	"	"	120.	"	"	"
-1.38	-1.89	0.51	"	"	150.	"	"	"
-3.67	-3.52	-0.15	"	150.	90.	"	"	"
-3.32	-3.70	0.38	"	"	120.	"	"	"
-2.93	-3.29	0.36	"	"	150.	"	"	"
-3.72	-3.05	-0.67	"	180.	90.	/	"	"
-3.74	-3.83	0.09	"	"	120.	/	"	"
-3.67	-3.83	0.16	"	"	150.	/	"	"
-2.08	-2.24	0.16	3.00	120.	90.	180.	"	"
-1.40	-1.70	0.30	"	"	120.	"	"	"
-0.87	-1.09	0.22	"	"	150.	"	"	"
-2.36	-2.03	-0.33	"	150.	90.	"	"	"
-2.06	-2.17	0.11	"	"	120.	"	"	"
-1.80	-1.96	0.16	"	"	150.	"	"	"
-2.30	-1.69	-0.61	"	180.	90.	/	"	"
-2.30	-2.26	-0.04	"	"	120.	/	"	"
-2.26	-2.31	0.05	"	"	150.	/	"	"
-0.89	-0.52	-0.37	4.00	120.	90.	180.	"	"
-0.55	-0.29	-0.26	"	"	120.	"	"	"
-0.28	-0.04	-0.24	"	"	150.	"	"	"
-0.96	-0.39	-0.57	"	150.	90.	"	"	"
-0.85	-0.49	-0.36	"	"	120.	"	"	"
-0.73	-0.44	-0.29	"	"	150.	"	"	"
-0.91	-0.26	-0.65	"	180.	90.	/	"	"
-0.96	-0.54	-0.42	"	"	120.	/	"	"
-0.96	-0.62	-0.34	"	"	150.	/	"	"

Water oligomers

Non-cyclic trimers $(H_2O)_3$

We computed stabilization energies of five non-cyclic trimer configurations[39] (Fig. 7), using our empirical potential with d(OH) = 0.9572 A, HOH = 104.52 degree. The results are listed in Table 7. Taylor[34] and Newton et al[39] calculated the energies of those configurations with an empirical potential and ab initio 4-31G calculations respectively. We recalculated the 4-31G values: $V_{ABC} = E_T - 3E_{mon} = \Sigma V^{(2)} + V^{(3)}$. These are listed in Table 7 to illustrate the basis set dependence. The difference in the values between each V_{ABC} of the ab initio result and the corresponding $\Sigma V^{(2)}$ of our potential result are the sums of nonadditive energies and the errors; these are related to the basis set chosen as reference. Our empirical parameters were obtained by fitting to 6-31G* calculated energies, so disagreement with the 4-31G calculations is not surprising.

Cyclic $(H_2O)_3$ with C_3 symmetry

The configurations used are shown in Fig. 8 and are the same as those used by Lentz et al..[25] The results from our empirical potential and from 6-31G* calculations, as well as those from Lentz[25] are listed in Table 8 for comparison. The monomer geometry is the same as that adopted by Lentz: d(OH) = 0.9450 A and HOH = 106 degree.

Since the optimized parameters were computed by consideration of pairwise interactions, no estimate of non-additive interactions were obtained. Non additive corrections, $V^{(n)}$, where n is equal to or larger than 3, were estimated for water oligomers on the basis of Lentzs' ab initio results.[25]

The three body non-additive energy, $V^{(3)}$, is calculated using the relationship: $V^{(3)} = E_T - 3E_{mon} - 3V^{(2)}$, where $V^{(2)}$ is the dimerization energy of an isolated pair. The differences between our total pairwise potential $3V^{(2)}$ and Lentzs' total pairwise $3V^{(2)}$ are as large as 6.22 kcal/mol. However, the differences between $3V^{(2)}$ calculated using our potential and the 6-31G* results are less than 3.2 kcal/mol. Since the optimized parameters of the new potential are based primarily on 6-31G* calculations (Of the 216 configurations 155 configurations were calculated with the 6-31G* basis set.), it is more reasonable to compare the empirical potential results with those computed using the 6-31G* basis. The differences between $3V^{(2)}$ from our 6-31G* ab initio calculations and those computed by Lentz are from 2.1 to 3 kcal/mol. These differences arise from the use of different basis sets and causes the empirical potential results to differ from that of Lentz by as much as 6 kcal/mol. However, the values of $V^{(3)}$ from our 6-31G* and Lentz' basis set differ by less than 0.2 kcal/mol. This indicates that, in the treatment of ice-h, it should be satisfactory to use Lentz's non-additive terms.

Table 7 Results for non-cyclic $(H_2O)_3$ (in kcal/mol)

	New Poten.[a]	6-31G*[a]		4-31G[a]	
	$V^{(2)}$	V_{ABC}	Dif.	V_{ABC}	Dif.
1.	-5.30	-6.26	-0.96	-10.26	-4.96
2.	-4.62	-5.63	-1.01	-8.85	-4.23
3.	-6.14	-6.80	-0.66	-10.96	-4.82
4.	-5.02	-5.51	-0.49	-9.10	-4.08
5.	-4.63	-5.03	-0.40	-7.89	-3.26

a. This work.
b. $V_{ABC}=E_T-3E_{mon}$

Configuration	1	2	3	4	5
r(H1-O1), A	.9572	.9572	.9572	.9572	.9572
r(H1-O2), A	2.15	2.15	1.95	1.95	1.95
r(H1-O3), A	2.15	2.15	2.50	2.50	2.50
HO1H1,deg	104.52	104.52	104.52	104.52	104.52
θ1, deg	135.	135.	150.	150.	150.
θ2, deg	132.	132.	132.	132.	132.
θ1',deg	135.	135.	110.	110.	110.
θ3, deg	132.	132.	132.	132.	132.
φ1, deg	180.	180.	180.	180.	180.
φ2, deg	0.	0.	0.	0.	0.
φ3, deg	180.	90.	180.	90.	0.
χ2, deg	90.	90.	90.	90.	90.
χ3, deg	90.	90.	90.	90.	90.

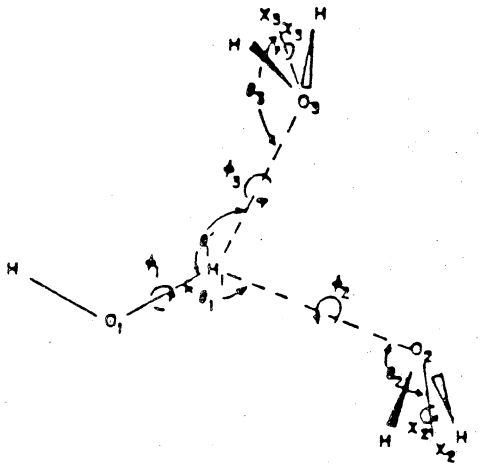

Fig. 7 Geometry of non-cyclic water trimer

Table 8 Results for C_3 cyclic $(H_2O)_3$ (in kcal/mol)

R(OO)	$3V^{(2)}$ [a]	6-31G*[a]		Lentz[b]	
A	Our Poten.	$3V^{(2)}$	Dif.	$3V^{(2)}$	Dif.
2.56	2.42	5.61	3.19	8.64	6.22
2.81	-7.47	-5.75	1.72	-2.73	4.74
3.00	-8.48	-7.95	0.53	-5.34	3.14
3.25	-7.29	-7.76	-0.47	-5.64	1.65

R(OO)	6-31G*[a]		Lentz[b]	
A	V_{ABC}	$V^{(3)}$	V_{ABC}	$V^{(3)}$
2.56	2.13	-3.48	4.98	-3.66
2.81	-7.17	-1.42	-4.24	-1.51
3.00	-8.74	-0.79	-6.18	-0.84
3.25	-8.18	-0.42	-6.10	-0.46

a This work.
b Reference 25.

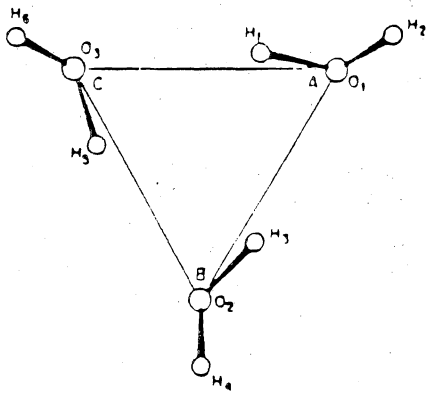

Fig. 8 Geometry of cyclic water trimer

Cyclic $(H_2O)_4$ with S_4 symmetry

The monomer geometry of the water tetramer shown in Fig. 9, is the same as that used for the cyclic C_3 trimer. Using the 6-31G* calculations of monomer energy, E_{mon}, tetramer energy, E_T, energies of isolated dimers, E_{AB} and E_{AC}, as well as isolated trimer energy, E_{ABC}, we calculated the total dimerization energy $V^{(2)}$, three-body interaction energy $V^{(3)}$ and four-body interaction energy $V^{(4)}$ through the following relationships:

$$V_{ABCD} = E_T - 4E_{mon}.$$

$$V^{(2)} = 4V_{AB}^{(2)} + 2V_{AC}^{(2)}.$$

where $V_{AB}^{(2)} = E_{AB} - 2E_{mon}$ and $V_{AC}^{(2)} = E_{AC} - 2Emon$

$$V^{(3)} = E_{ABC} - 2E_{AB}^{(2)} - E_{AC}^{(2)}$$

$$V^{(4)} = V_{ABCD} - 4V_{AB}^{(2)} - 2V_{AC}^{(2)} - 4V^{(3)}.$$

where $V_{AB}^{(2)}$ or $V_{AC}^{(2)}$ is the dimerization energy of the isolated pair AB or AC.

As seen in Table 9, the differences between the total $V^{(2)}$ computed from the empirical potential and from the 6-31G* basis are less than 3 kcal/mol. In Tables 8 and 9 the pairwise empirical potential energies are shown to deviate from the results of 6-31G* by around 3 kcal/mol. This is the result of accumulated errors. For the dimer, the error is only about 0.5 kcal/mol. Since the total pairwise energy for an S_4 tetramer in the potential calculation is composed of four pairwise AB energy values and two pairwise AC energy values (see Figure 9), the accumulated error could be as high as 3 kcal/mol. The small differences between $V^{(3)}$ and $V^{(4)}$ of the 6-31G* basis and those of Lentz again suggests it is reasonable to estimate non-additive energies directly from Lentzs' data.

Table 9 Results for S_4 configuration of $(H_2O)_4$ (in Kcal/mol)

R(OO)	$V^{(2)}$	6-31G*[a]		Lentz[b]	
A	New Poten.	$V^{(2)}$	Dif.	$V^{(2)}$	Dif.
2.80	-22.81	-23.12	-0.31	-19.58	3.23
3.00	-22.11	-23.89	-1.78	-20.88	1.23
3.15	-19.96	-22.41	-2.45	-19.76	0.20

R(OO)	6-31G*[a]			Lentz[b]		
A	V_{ABCD}	$V^{(3)}$	$V^{(4)}$	V_{ABCD}	$V^{(3)}$	$V^{(4)}$
2.80	-27.73	-1.06	-0.37	-23.66	-0.95	-0.28
3.00	-26.84	-0.68	-0.23	-23.36	-0.58	-0.16
3.15	-24.59	-0.51	-0.16	-21.51	-0.41	-0.12

a This work.
b Reference 25.

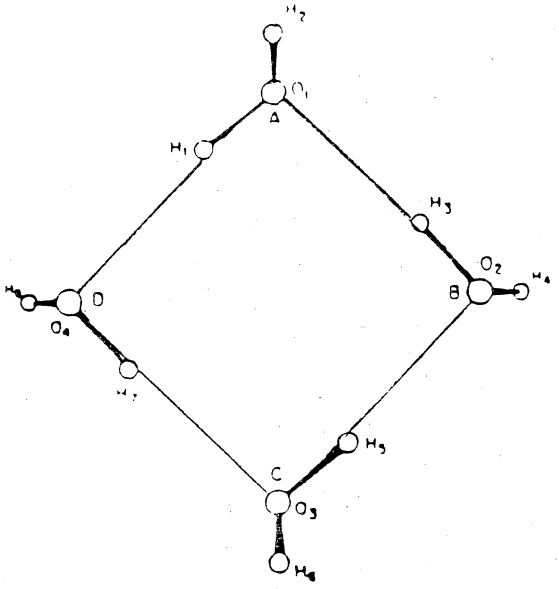

Fig. 9 Geometry of water tetramer

Ice-h

The lattice energy of ice-h has been estimated from experimental data to be -13.4 kcal/mol[20]. In ice-h, each oxygen is surrounded by four oxygen atoms in the first neighbouring layer. The four oxygen atoms are oriented in a near tetrahedral configuration. Each H_2O makes four H-bonds with the nearest oxygen atoms; two protons comes from the central oxygen and the other two protons from neighbouring H_2Os. Pauling[40,41] hypothesized the six possible combinations have equal probability. The lattice energy of ice-h is calculated on the basis of this hypothesis. The H-bonding energy of ice-h can be defined as one half of the lattice energy of a mole of ice. This is one of several H-bonding definitions[22] for ice.

The space group of ice-h is D_{6h}^4 -C6/mmc.[41] From the neutron diffraction of D_2O, d(O-D) = 1.01 A. d(O-O) = 2.76 A and the angle among any three neighbouring oxygen atoms are 109.63 degree if two of the three oxygens are along the crystal c axis and 109.31 degree if no two oxygen atoms are along the c axis.[20] From proton magnetic resonance studies, d(H-H) = 1.584 A.[42] For simplicity, we have adopted regular tetrahedral configurations for the empirical calculations. We used d(O-O) = 2.76 A and d(O-H) = 1.0 A in our calculations.

The lattice surrounding an arbitrary oxygen atom has the following structure: The four oxygens in the first layer are at a distance of d(O-O) = 2.76 A from the central oxygen. In the second layer

there are twelve oxygens with d(O-O) = 4.51 A; three above the central oxygen along the c axis, and three below. The remaining six and the central oxygen are in a plane perpendicular to the c axis. Only one oxygen with d(O-O) = 4.60 A is in the third layer. Because the values of d(O-O) for the second and the third layers are similar, Lentz et al. included the single H_2O of the third layer as a part of the second layer. Interactions from the fourth layer and beyond are neglected both in our calculations as well as those of Lentz et al..

First Layer Lattice Energy

The H_2O along c in the first layer has its hydrogens eclipsed with those of the central H_2O. The remaining H_2Os have staggered hydrogen configurations. There are three eclipsed configurations for the oxygen along the c axis. Each of the other three oxygens has three staggered configurations. Therefore, there are a total of three eclipsed and nine staggered configurations. In accordance with Pauling's hypothesis, we assumed that each of the twelve configurations occurs with the same probability. Using Pauling's hypothesis to determine the weighting factors, the average $V_{AB}^{(2)}$ for the first layer is -5.11 kcal/mol in the empirical calculation. The total first layer lattice energy, which is one half of the $4 \bullet V_{AB}^{(2)}$ interactions, is -10.23 kcal/mol.

Calculations were also carried out for this layer using the 6-31G* basis set for comparison. The result is -4.49 kcal/mol for the average $V_{AB}^{(2)}$, i.e. -9.0 kcal/mol for the total first layer lattice energy.

For the first layer energy, the 6-31G* results (this work), the empirical results (this work) and the results of Ben-Naim Stillinger potential[5] are listed in Table 10. The empirical result (-10.1 kcal/mol) is much lower than Lentzs' value (-6.5 kcal/mol) and should be higher than that calculated from Ben-Naim Stillinger's potential. However, it is close to the results calculated using a 6-31G* basis set.

Second Layer Lattice Energy

In the pairwise calculations involving the second layer, we use AA and DD to specify the non-sequential relation between two oxygens in the second layer where both oxygens are either proton acceptors or proton donors. AD and DA are sequential configurations and are specified for configurations where one of the two oxygens is a proton acceptor and the other a proton donor. Among the twelve oxygens in the second layer the six above or below along the axis c are staggered relative to the central oxygen. The six in the same plane with the central oxygen are eclipsed.

For the staggered configurations, we calculated pairwise energies separately for AA, DD, AD and DA. For each of the four cases there are nine configurations. So, there are a total of thirty six configurations for the staggered cases. Similarly, there are another thirty six configurations for the eclipsed.

In the case of AD or DA of the second layer, each oxygen in the first layer has four neighbouring oxygens: a,b,c,d. In the second layer relationship, a-O-c, the oxygen of the first layer accepts a proton from a and donates a proton to c. The second proton of this H_2O can donate to either b or d. There is one AA, one DD, two AD and another two DA configurations. For each of the staggered and the eclipsed cases there are six A and D combinations. Again, equal probability is assumed for each of the twelve combinations. Using these weighting factors, the total second layer lattice energy, equal to one-half of the $12 \bullet V_{AC}^{(2)}$ interactions, is -1.2 kcal/mol. This is composed of two non-sequential interaction energies $V_{AC}^{(2)} = +2.04$ kcal/mol and four sequential $V_{AC}^{(2)} = -3.28$ kcal/mol. The corresponding value of the energy reported by Lentz, including the single third layer H_2O, is -2.1 kcal/mol.

Table 10 Energy comparison for the first layer of ice-h

		6-31G*[a]	Emp.[a]	Ben-Naim[b]
Eclipsed	180	-5.28	-5.56	-6.50
	± 60	-4.09	-4.74	-5.58
Staggered	±120	-4.75	-5.26	-6.13
	0	-3.99	-4.57	-5.34

a. This work. in Kcal/mol.
b. Reference 5 in Kcal/mol.

Third Layer Lattice Energy

Only one oxygen atom is in the third layer, 4.60 A from the central oxygen atom. Although there are 6 distributional possibilities for each pair of protons belonging to an oxygen located in the center of a tetrahedron and 36 possibilities for such a pair of oxygen atoms in the third layer, once the water dimer is isolated from the crystal, twelve configurations suffice to describe the interactions. Using weighting factors based on the above arguments, we computed $V_{AD}^{(2)}$ to be + 0.026 kcal/mol. The third layer lattice energy contrubution is one half of this value: + 0.013 kcal/mol.

The lattice energy of ice-h approximated to the third layer as expressed by Lentz et al.[25] is:

$$E_{ice} = 2(V_{AB}^{(2)})_{av} + 4(V_{AC}^{(2)} + V_{ABC}^{(3)})_{avseq} + 2(V_{AC}^{(2)} + V_{ABC}^{(3)})_{avnonseq} + 2V_{AB}^{D} + 6V_{AC}^{D}.$$

The results calculated from our empirical potential and Lentzs' ab initio results[25] are listed in Table 11. The non-additivity contributions, taken directly from Lentz et al., is -4.36 kcal/mol. The lattice energy of ice-h calculated from our empirical potential using Lentzs' value for the non-additivity contributions is -15.6 kcal/mol. Lentzs' result is -12.9 kcal/mol. These calculated results bracket the estimated experimental value of -13.4 kcal/mol.[22] In contrast, the lattice energy calculated using CNDO/2 is -4.9 kcal/mol.[43]

Table 11 Lattice Energy of Ice-h
(in kcal/mol)

	Empirical	6-31G*	Lentzs'	Exp.
1st layer	-10.06	-8.99	-6.46	
2nd layer				
Non seq.	+2.04		+2.06	
Seq.	-3.28		-4.16	
3rd layer	+0.01		Included in 2nd layer.	
Three body interaction	-4.36 (from Lentzs')		-4.36	
Total	-15.6		-12.9	-13.4

The first layer

1 eclipsed xoox' = 180 °
= ± 60 °
3 staggered xoox' = ± 120 °
= 0 °

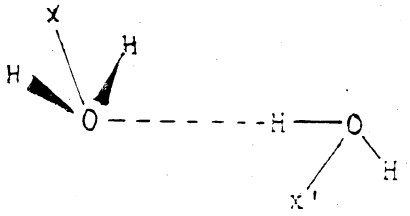

The second layer
S-sequential
A-proton accepted

N-non sequential
D-proton doner

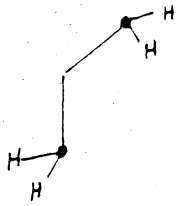
9NAA

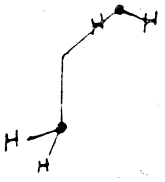
9SAD

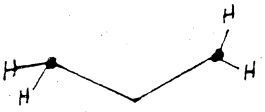
9NAA

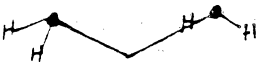
9SAD

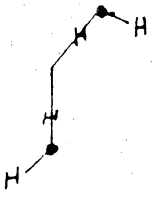
9NDD

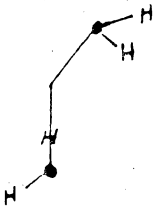
9SDA

Staggered

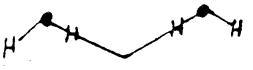
9NDD

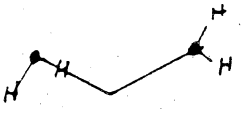
9SDA

Eclipsed

The third layer

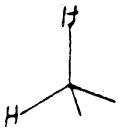

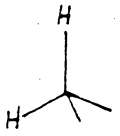

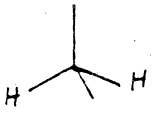

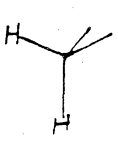

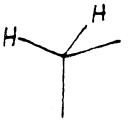

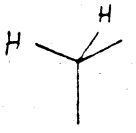

A type-3 B type-6 C type-3

Fig. 10 Pairwise relationship in lattice ice-h

Methanol crystal, β-modification

An IR study of the shift of the O-H vibration frequency[44] led to an estimate of -7.5 kcal/mol for the strength of the hydrogen bonds in methanol.

We applied our pairwise empirical potential to the β modification of methanol and calculated a value of -7.9 kcal/mol for the lattice energy. Only pairwise relationships among the monomers in the crystal were considered. The cut-off lengths are taken to be the same as the parameter a of the orthorombic unit cell. To obtain the appropriate distances, we made use of the coordinates of the carbons and oxygens based on the results of X-ray diffraction.[45] The coordinates of hydrogen atoms were based on our optimization result of a 6-31G* basis calculation of the methanol monomer. Their cartesian coordinates in Angstrom are listed in the Appendix A. Listed below are the five kinds of pairwise interactions considered:

E(AB) = -2.13 kcal/mol x(1/2) x 2 neighbors

E(AB′) = -1.11 kcal/mol x(1/2) x 2 neighbors

E(AG) = -1.48 kcal/mol x(1/2) x 4 neighbors

E(AD) = -0.84 kcal/mol x(1/2) x 2 neighbors

E(AD′) = -0.84 kcal/mol x(1/2) x 2 neighbors

The molecules A, B and B′ are located in the plane a = 0. (The a, b and c are the parameters of the orthorombic unit cell.) The molecules D and G are in a plane at (1/2)a. The relationships among the molecules A, B, B′, D, D′ and G are shown in Fig. 11. The lattice energy, which is the sum of the cited energies, is -7.9 kcal/mol.

$$E(\text{lattice}) = E(AB) + E(AB') + E(AG) + E(AD) + E(AD').$$

This value is close to the experimental hydrogen bonding energy of methanol determined in the O-H vibration frequency study mentioned earlier.

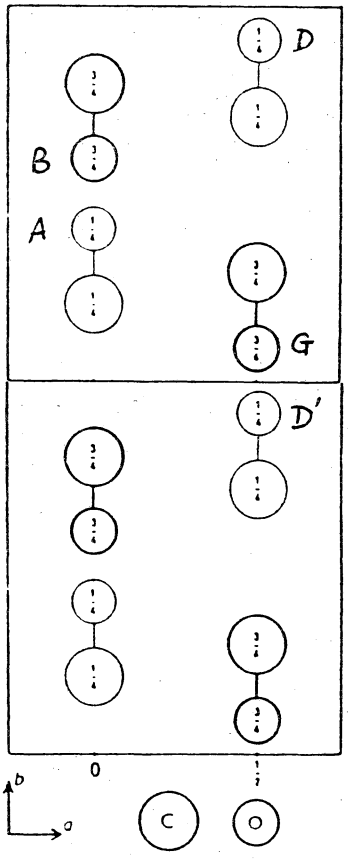

Figure 11. Structure of the β-methanol crystal, projected along the c-axis of the orthorhombic cell.

Conclusion

1. The empirical potential used in this thesis is composed of two parts: electrostatic interactions and van der Waals interactions. The van der Waals interactions are the same as those used in Allinger's molecular mechanics program, MM2.[18b] Point charges models were used for the electrostatic interactions. The parameters of the point charge models were optimized through a simplex optimization program to fit the empirical results to ab initio results (6-31G* basis set and MCYs' CI calculations). Neither Morse terms nor the orientations of the dipoles were involved in our empirical potential. Therefore, our potential is simpler than Taylor's[3a] and Kroon's[4], which do use these terms in their potentials.

2. Comparison of the results of the empirical potential, the experimental results and those of 6-31G* ab initio calculations for several cases of water oligomers, ice-h and the ammonia dimer showed that the differences are ca. 1 kcal/mol for the various dimerization energies. The empirical potential can be applied to calculate reasonable pairwise stability energies of water oligomers and ammonia dimers.

3. The results from the empirical potential are comparable to those from 6-31G* calculations. When compared to the results of other basis sets, the differences between the results of 6-31G* and

those of the other basis set must be taken into account. The empirical potential is for interactions of pairs of monomers and non-additive interaction energies are not computed.

4. The potential is compatible with the MM2 program.

5. The local H-bonding energies of a large molecule can be estimated with the empirical potentials. Extensions should be applicable to consideration of H-bonding in carbohydrates and polypeptides.

Determination of the Orientation of Anthracene Molecules in the Unit Cell by means of a Refractivity Method

Introduction

The dependence of a crystal's refractive indices on the structure and orientation of its constituent molecules has been exploited in several different ways. Bragg[46a,46b] and Zachariasen[47] calculated the refractive indices of calcite, aragonite and sodium bicarbonate crystals from their atomic arrangements. On the basis of the birefringence in calcite and sodium nitrate crystals, Bragg[46b] determined the bond distance for N-O. Bhagavantam[48a,48b] determined the magnetic and optical properties of aromatic compounds and attempted to relate the properties to the orientation of the molecules in the crystal lattice. For anthracene, using the molecular structure and its orientation from X-ray diffraction, Julian and Bloss[49] calculated the molecular refractivities from the refractive indices of the crystal. Bunn[50] calculated its crystal refractive indices from the directional bond polarizabilities of the molecular bonds. The purpose of the present study is to illustrate the reverse procedure; we investigate the possibility of determining the molecular orientation in the unit cell by matching the macroscopic optical properties of the crystal to those calculated from a molecular structure.

The macroscopic directional refractivities of the crystal, the density, the point/space group of the crystal and the crystal constants as well as the molecular structure are assumed to be known. Starting with empirical bond polarizabilities, we use the simplex method to optimize the molecular orientation by matching the orientation and shape of the crystal refractivity ellipsoid. While our

calculation is confined to anthracene, the idea can be extended to any other monoclinic crystal without difficulty. In fact, except for the cubic system with isotropic properties, this method should also be capable of extension to other crystal systems.

Method

To illustrate the method we use an approximate molecular geometry for anthracene in which the aromatic rings are assumed to be regular hexagons, and all bond angles are taken to be 120°. Figure 12 shows the idealized molecular geometry and indicates the directions (l,m,n) of the principal components of its polarizability tensor. We employ the standard longitudinal (P_l) and transverse (P_t) bond polarizabilities listed in Table 12 and calculate the three principal components of molecular polarizability by summing over all bonds, b:

$$p_i = \sum_b (P_l(b) \bullet \cos^2 A_{bi} + P_t(b) \bullet \sin^2 A_{bi}), \ (i = l,m,n) \tag{1}$$

where A_{bi} is the angle between the bth bond and the ith axis. The principal molar refractivities are then calculated from

$$r_{ii} = (4\pi/3) N p_i, (i = l,m,n) \tag{2}$$

where N is Avogadro's number. The values obtained for anthracene are:

$$r_{ll} = 76.4 cc/mole \ r_{mm} = 69.7 cc/mole \ r_{nn} = 34.5 cc/mole.$$

To describe the crystal refractivities, we use an orthogonal coordinate system (a′,b′,c′), where a′ and b′ are chosen parallel to the crystal axes a and b, and c′ is taken to be perpendicular to a′ and b′. For simplicity, (a,b,c′) is used to express (a′,b′,c′). If we use u_{jk} to represent the direction cosine of unit vector j with respect to the direction k, and note that $u_{jk} = u_{kj}$, we can use the following orthogonal transformation to transform the molecular refractivities to the (a,b,c′) coordinate system:

$$R = \begin{bmatrix} u_{al} & u_{am} & u_{an} \\ u_{bl} & u_{bm} & u_{bn} \\ u_{c'l} & u_{c'm} & u_{c'n} \end{bmatrix} \begin{bmatrix} r_{ll} & 0 & 0 \\ 0 & r_{mm} & 0 \\ 0 & 0 & r_{nn} \end{bmatrix} \begin{bmatrix} u_{la} & u_{lb} & u_{lc'} \\ u_{ma} & u_{mb} & u_{mc'} \\ u_{na} & u_{nb} & u_{nc'} \end{bmatrix} \tag{3}$$

The anthracene crystal has symmetry $P2_1/a$. The two molecules in the unit cell differ in orientation only with respect to the signs of u_{lb} , u_{mb} and u_{nb}; the magnitudes of these as well as the magnitudes and signs of the other direction cosines are identical for the two molecules. When one averages the result of equation (3) for the two molecules in the unit cell the following is obtained for the molar refractivity of the crystal:

$$R = \begin{bmatrix} \sum_j r_{jj} \bullet u_{ja}^2 & 0 & \sum_j r_{jj} \bullet u_{ja} u_{jc'} \\ 0 & \sum_j r_{jj} \bullet u_{jb}^2 & 0 \\ \sum_j r_{jj} \bullet u_{ja} \bullet u_{jc'} & 0 & \sum_j r_{jj} \bullet u_{jc'}^2 \end{bmatrix} \tag{4}$$

where j = l,m,n. The four zeroes arise from the sign changes in u_{lb} , u_{mb} and u_{nb} noted earlier. The form of this matrix is typical of second order tensor properties for monoclinic crystals (Sands[51]). Diagonalization of this matrix yields three principal refractivities as the eigenvalues. The direction cosines of the principal axes relative to a, b, and c′ are obtained from the eigenvectors. The calculated matrix has a trace of 180.60, while the sum of the three principal refractivities from experiment (Julian and Bloss[49]) is 187.97. The difference between these numbers reflects errors in the approximate molecular structure and in the empirical bond polarizabilities employed. This slight error will make exact predictions of molecular orientations impossible.

For each set of assumed molecular orientations a corresponding resultant ellipsoid can thus be calculated. For the monoclinic crystal the orientation of this ellipsoid in three dimensional space is described by an angle between c′ and the longest principal axis. The difference between the experimental and the calculated angles can be used as one standard for optimization of the molecular orientation in the unit cell. For anthracene $\beta = 124.7°$, $U = 7.5°$ (the angle between the longest principal semi-axis and the monoclinic c), so the experimental angle from c′ is 27.2°. In addition we can compare the shapes of the calculated and experimental ellipsoids as measured by the ratios R_2/R_1 and R_3/R_1. Here R_1 is the smallest eigenvalue and R_2 is the largest. For anthracene the ratios of the principal semi-axes of the experimental refractivity ellipsoid are $R_2/R_1 = 1.805$ and $R_3/R_1 = 1.348$.

A linear combination of these standards with different weighting factors (C_i) yields a function F which can be minimized to determine the correct molecular orientation:

$$F = C_1 | \Delta | + C_2 | 1.805 - (R'_2/R'_1)_{cal} | + C_3 | 1.348 - (R'_3/R'_1)_{cal} | \qquad (5)$$

Δ is the deviation between the experimental angle, 27.2°, and the calculated one.

Since the nine direction cosines for a molecule must satisfy the usual orthonormality conditions (Nye[52]), only three out of the nine are independent. We chose u_{la} , u_{lb} and u_{ma} as the independent parameters. These must satisfy the consistensy conditions:

$$u_{la}^2 + u_{lb}^2 \leq 1$$

and

$$u_{la}^2 + u_{ma}^2 \leq 1$$

to ensure that all direction cosines are real. For each choice of these three, we solved the orthonormality equations for the remaining direction cosines and used equation (4) to obtain the crystal refractivity tensor. Because of the quadratic nature of the orthonormality equations, this

procedure gives eight different solutions, four of which refer to the orientation of each molecule in the unit cell. The four solutions for each molecule are related to one another by a reflection through the (a,b) plane and a second reflection through the (l,m) plane.

Optimization of the Molecular Orientation

A simplex algorithm (O'Neill[15]) was used to minimize F (eq. (5)) with respect to the orientation of the anthracene molecules. In practice we found that there are an infinite number of ellipsoidal orientations with zero Δ, which indicates that the orientation condition as reflected in Δ is a weaker condition and the first term of eq. (5) should receive relatively little weight. Best results were obtained with $C_1 = 0.02$ and $C_2 = C_3 = 1.0$.

Table 13 lists the three starting angle set and the optimized angle set for several calculations. The errors between the actual orientation and the calculated orientation of anthracene molecules in the unit cell differ by less than 10°. The optimized angle sets with F less than or equal to 0.088 appear to represent reasonable results. For most starting sets chosen, initial step angles of 30° were found to be suitable for optimization.

This method can be used for other monoclinic molecular crystals. It should also be possible to apply this optimization method of molecular orientation to other crystal systems with the exception of the cubic system with isotropic molecular properties. It may also be useful in studies of optical properties of liquid crystals.

Table 12 Parameters for Bond Polarizabilities (from Ref. 50, p313)

	$10^{25} x P_l / cm^3$	$10^{25} x P_t / cm^3$
C-C (aromatic)	22.5	4.8
C-H	8.2	6.0

Table 13 Optimized Angle Set of Anthracene Molecules in their Monoclinic Unit Cell

Start angles are l_a, l_b and m_a.

Optimized angle set is expressed as following matrix form:

$$\begin{matrix} l_a & l_b & l_{c'} \\ m_a & m_b & m_{c'} \\ n_a & n_b & n_{c'}. \end{matrix}$$

The actual angle set for 1st molecule in the unit cell is:

119.70	97.10	30.71
108.86	153.19	108.34
36.27	115.71	66.28.

That for 2nd molecule in the unit cell is:

119.70	83.00	30.68
108.86	26.73	108.23
36.27	64.34	66.23.

				Remarks
Start angles	5.00	87.00	85.00	
Step angles	30.00	30.00	30.00	
Weighting factors	0.02	1.00	1.00	
F	0.085			
Δ	0.000			
R2 R3 R1	76.400	59.803	44.397	
R2/R1 R3/R1 R2/R3	1.7208	1.3470	1.2775	
Optim. angle set	62.93	89.74	152.93	
	61.71	147.98	76.24	
	41.08	57.98	67.17	
Equivalent angle	117.07	90.26	27.07	2nd
set	118.29	32.02	103.76	molecule
	41.08	57.98	67.17	
Start angles	90.00	90.00	90.00	
step angles	30.00	30.00	30.00	
Weighting factors	0.02	1.00	1.00	
F	0.085			
Δ	-0.000			
R2 R3 R1	76.400	59.802	44.398	
R2/R1 R3/R1 R2/R3	1.7208	1.3470	1.2775	
Optim. angle set	117.19	90.02	27.19	
	61.85	147.98	75.99	
	138.94	122.02	112.80	
Equivalent angle	117.19	90.02	27.19	2nd
set	118.15	32.02	104.01	molecule
	41.06	57.98	67.20	

Table 13 Optimized Angle Set of Anthracene Molecules in their Monoclinic Unit Cell (continued)

				Remarks
Start angles	92.00	92.00	92.00	
Step angles	30.00	30.00	30.00	
Weighting factors	0.02	1.00	1.00	
F	0.084			
Δ	-0.000			
R2 R3 R1	76.400	59.841	44.359	
R2/R1 R3/R1 R2/R3	1.7223	1.3490	1.2767	
Optim. angle set	117.20	90.00	27.20	1st
	118.08	148.05	104.00	molecule
	41.01	121.95	67.18	
Start angles	179.00	88.00	88.00	
Step angles	30.00	30.00	30.00	
Weighting factors	0.02	1.00	1.00	
F	0.088			
Δ	-0.003			
R2 R3 R1	76.338	59.837	44.424	
R2/R1 R3/R1 R2/R3	1.7184	1.3470	1.2758	
Optim. angle set	240.53	85.20	29.94	
	64.66	147.51	71.06	
	139.30	122.04	112.28	
Equivalent angle	119.47	85.20	29.94	2nd
set	115.34	32.49	108.94	molecule
	40.70	57.96	67.72	
Start angles	87.00	87.00	87.00	
Step angles	30.00	30.00	30.00	
Weighting factors	0.02	1.00	1.00	
F	0.084			
Δ	0.000			
R2 R3 R1	76.400	59.841	44.359	
R2/R1 R3/R1 R2/R3	1.7223	1.3490	1.2767	
Optim. angle set	117.20	90.01	27.20	1st
	118.08	148.05	104.00	molecule
	41.00	121.95	67.18	

Table 13 Optimized Angle Set of Anthracene Molecules in their Monoclinic Unit Cell (continued)

				Remarks
Start angles	30.00	60.00	90.00	
Step angles	30.00	30.00	30.00	
Weighting factors	0.02	1.00	1.00	
F	0.084			
Δ	0.000			
R2 R3 R1	76.400	59.841	44.359	
R2/R1 R3/R1 R2/R3	1.7223	1.3490	1.2767	
Optim. angle set	62.80	90.00	152.80	
	118.08	148.05	104.00	
	139.00	58.05	112.82	
Equivalent angle	117.18	90.00	27.20	1st
set	118.08	148.05	104.00	molecule
	41.00	121.95	67.18	
Start angle	22.00	76.00	88.00	
Step angle	30.00	30.00	30.00	
Weighting factors	0.02	1.00	1.00	
F	0.085			
Δ	0.000			
R2 R3 R1	76.400	59.802	44.398	
R2/R1 R3/R1 R2/R3	1.7208	1.3470	1.2775	
Optim. angle set	62.80	90.00	152.80	
	61.86	147.98	75.97	
	41.06	57.98	67.20	
Equivalent angle	117.20	90.00	27.20	2nd
set	118.14	32.02	104.03	molecule
	41.06	57.98	67.20	

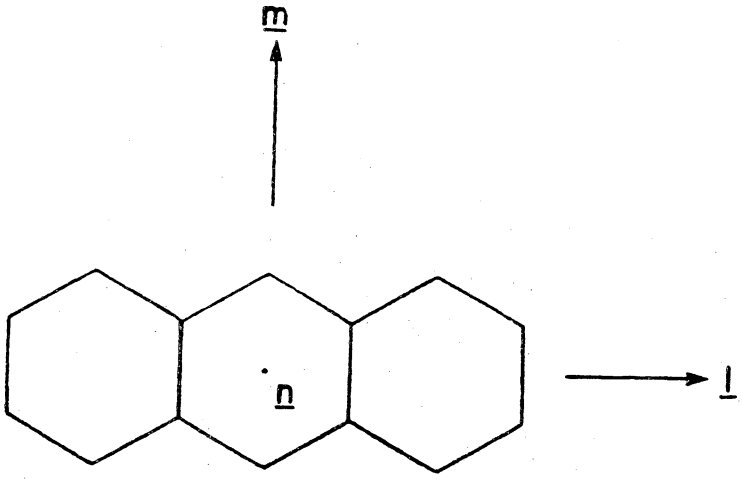

Fig. 12. The principal axis system of anthracene

Some Ab Initio Calculations Involving The Acetonitrile Exchange Reaction

Introduction

Acetonitrile has been used as a solvent in reactions which introduce labelled carbon isotopes into organic compounds. However, significant loss of the radioactivity of the products was found by Jay et al.[6] This led them to postulate the following exchange reaction:

$$CH_3CN + \overset{*}{C}N^- = CH_3\overset{*}{C}N + CN^-.$$

A mixture of KCN labelled with carbon 13, normal acetonitrile and crown ether (18-crown-6) were refluxed. When the distillate was analyzed with NMR and MS, they found an enrichment of carbon-13 in the nitrile carbon of the acetonitrile.

They suggested that a mechanism involving addition-rearrangement-elimination processes, scheme 1 in Fig. 13, was more likely than a S_N2 mechanism (scheme 2, Fig. 13). Their reasoning was that the cyanide anion is a good nucleophile but the cyano function is a poor leaving group in the S_N2 sense and nucleophiles such as hydroxide, alkoxides, amines and sodamide are known to attach to the electrophilic carbon atom resulting in additions to the $C \equiv N$ bond rather than in S_N2 displacement of the cyano group.[53] Examples cited to support their arguments include: 1. A Grinard reagent reaction with cyano functional group[54] undergoes an addition rather than a displacement, 2. Benzilic acid undergoes an analogous rearrangement[55a] and 3. The benzoin condensation results in a loss of the cyanide ion.[55a]

A new and revised mechanism (scheme 3 in Fig. 13) was suggested by Andrade et al.[7] Based on the results of their MNDO calculations, they showed that this mechanism is a more likely candidate. This is a prototropic type mechanism via a cyclopropane intermediate. Starting at a precusor (1), precusor (5) is formed through a 1,3 hydrogen shift. Although the prototropic shift is forbidden[56,57] in the gas phase, it is thought to occur rapidly in solution by stepwise proton transfers.[55b]

Based on 4-31G and 3-21G basis 'ab initio' calculations, we arrive at the contrary result that the S_N2 mechanism (scheme 2) is the most likely among the three mechanisms suggested. In the MNDO results, the precusor (3) of scheme 2 has the hightest energy level but the lowest activation energy. In order to determine which of the two factors plays the predominant role, a simple kinetic treatment was used. It is based on a Boltzmann distribution of the precusor concentrations and the Arrhenius law for the rate equation. The three mechanisms were treated as concurrent pathways. The activation energy of the process from (1) to (5) is ignored. The assumption is made that the concentrations of the three precusors reach an equilibrium instantly. Based on this treatment and the MNDO and 4-31G results, we conclude that the Walden inversion mechanism predominates over the mechanism shown in scheme 1. Even though the mechanism shown in scheme 3 predominates over the Walden inversion in the MNDO results, our 4-31G calculations show the reverse. For the precusors and the intermediate, we optimized all the structural parameters in our 4-31G calculations while only part of the parameters were optimized in the cited MNDO report.[7]

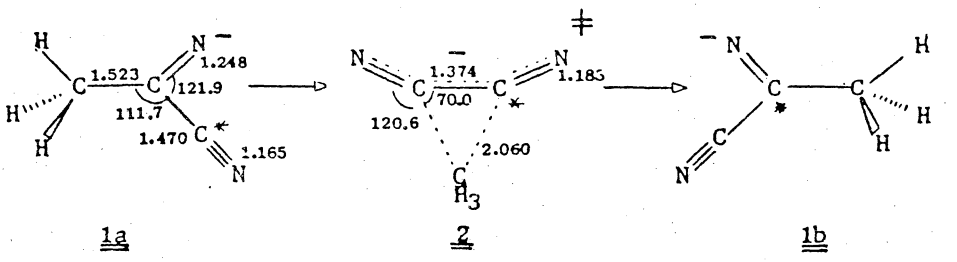

1a 2 1b

Scheme 1

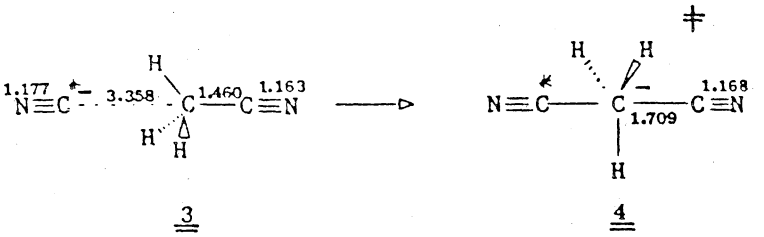

3 4

Scheme 2

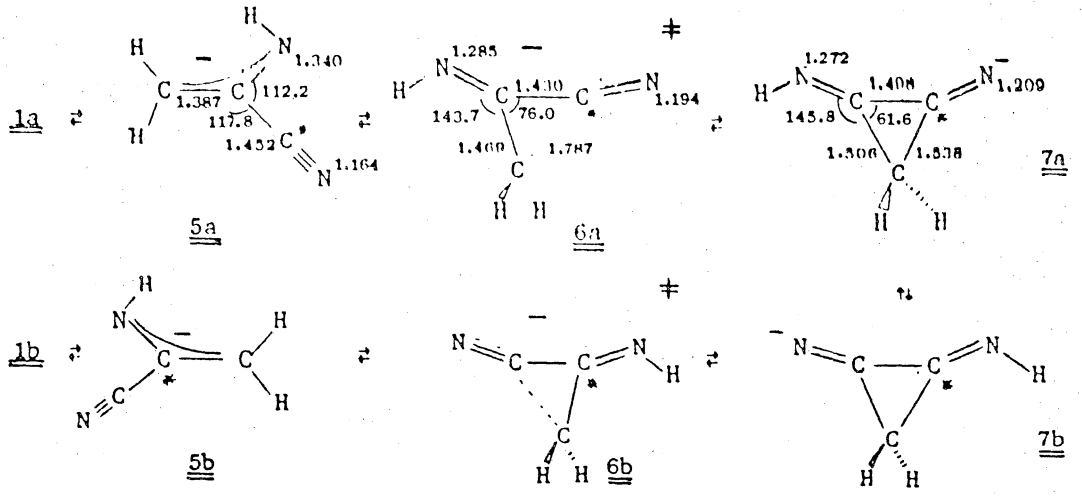

Scheme 3

Fig. 13. Mechanisms suggested for the acetonitrile exchange reaction

Results

The geometrical parameters of all structures except for transition states (TS2) in scheme 1 and (TS6) in scheme 3, have been completely optimized. Due to the excessive cpu time needed for the computer calculation and the difficulty of reaching a convergent geometry for a transition state (a saddle point of the potential energy surface with all force constants positive except one), only six parameters were optimized in TS2. The structures are shown in Table 14. The energy levels of the different precursor structures, the transition state structures and the intermediate structures are shown in Fig. 14. Treated as a S_N2 mechanism, Viers et al.[58] obtained the same MNDO results as Andrade et al. did. and Wolfe et al.[59] reported the same 4-31G results for the S_N2 mechanism as we did.

Assumptions made were: 1. The relative energy relationships calculated using MNDO or the 4-31G basis set in the ab initio calculations maintains its validity at 298K. Zero point energy contributions were not included; 2. Solvation effects were neglected and the reaction is treated as a first order reaction; 3. The frequency factors are assumed to be of the same order of magnitude for the three mechanisms. In addition, the activation energy from (1) to (5) is ignored and concentrations of the three precusors are assumed to reach equilibrium instantly as stated earlier. Using these assumptions, it is possible to calculate the concentration ratios and the ratios of the reaction rates at 298K.

$$\frac{C_2}{C_1} = \frac{e^{\frac{-E_2}{RT}}}{e^{\frac{-E_1}{RT}}} = e^{\frac{E_1 - E_2}{RT}}$$

$$v_i = \frac{-dC_i}{dt} = C_i A_i e^{\frac{-\Delta E_i}{RT}}$$

$$\frac{v_2}{v_1} = e^{\frac{E_1 - E_2 + \Delta E_1 - \Delta E_2}{RT}}$$

where C_i is the concentration of ith precusor, E_i the energy level of the ith precusor, A_i the frequency factor of the ith mechanism and ΔE_i the activation energy for the ith precusor.

When MNDO energy levels were used for the three precusors 1, 3 and 5, the concentration ratios at 298K can be calculated. Combining these concentration ratios with the Arrhenius law, we calculated the ratios of the reaction rates as follows:

$$v_2 : v_1 = 24.7$$

$$v_2 : v_3 = 3.3 \bullet 10^{-11}$$

where v_2 is the rate of scheme 2 etc..

When 4-31G energy levels of the precusors were used for the calculation, the ratios are:

$$v_2 : v_1 = 2.6 \bullet 10^{22}$$

$$v_2 : v_3 = 1.3 \bullet 10^{35}.$$

Based on the MNDO energy levels and the rate estimation, the Walden inversion mechanism predominates over the mechanism of the scheme 1. Based on the 4-31G results and the rate estimation, the Walden inversion mechanism predominates over both those mechanisms of the scheme 1 and scheme 2. We compare them further in the next section.

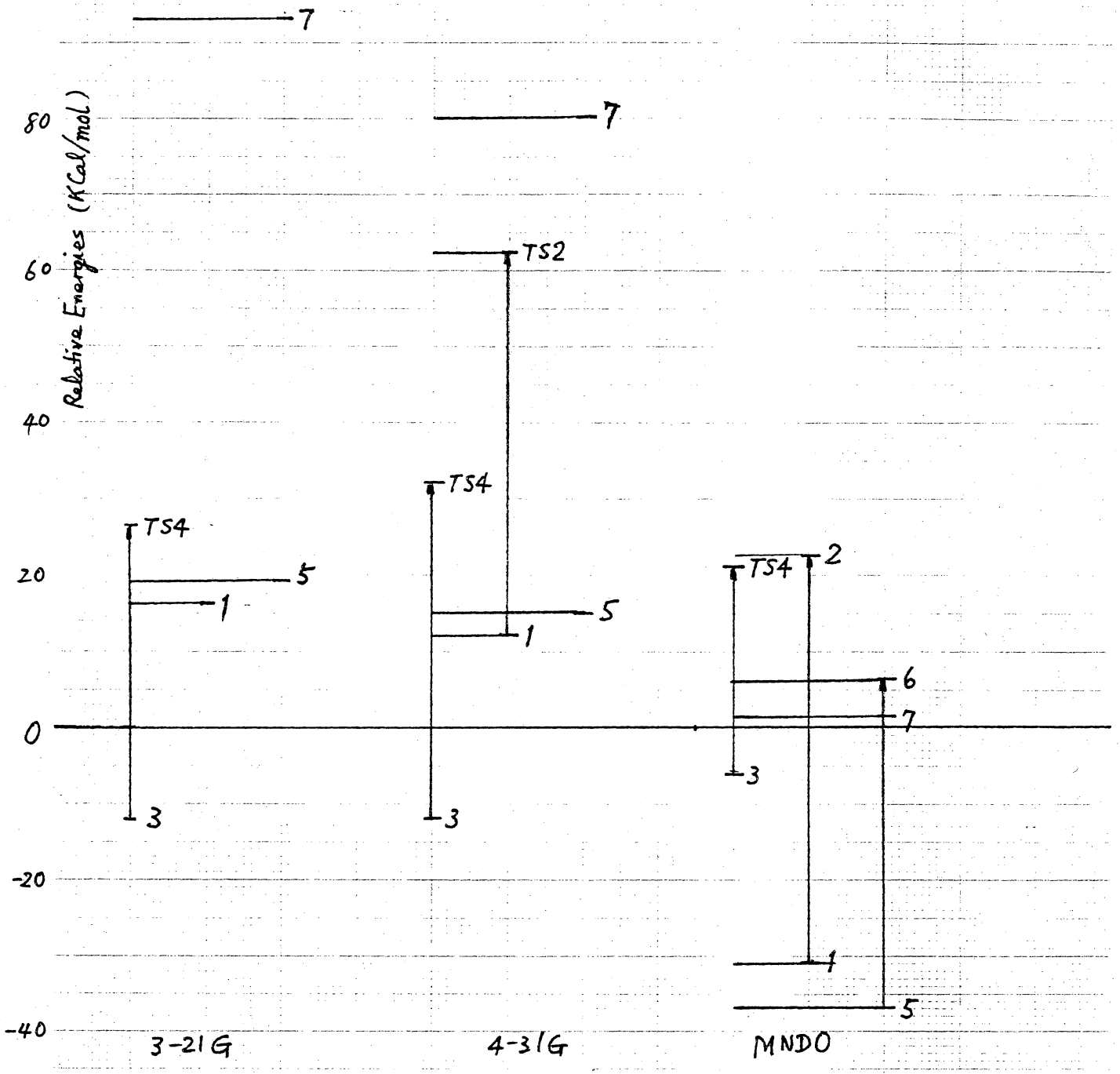

Fig. 14 Energy levels of the precusors, the intermediate and the transition states

Table 14 Optimized Geometrical Parameters and Energy Values

Data with * are fixed parameters. Units in A or deg..

Structure 1			Structure 3		
Basis set	3-21G	4-31G	Basis set	3-21G	4-31G
C1N1	1.25	1.25	C1N1	1.14	1.14
C3C1	1.55	1.53	C2C1	1.46	1.46
H1C3	1.08	1.08	H1C2	1.08	1.08
H2C3	1.09	1.09	H2C2	1.08	1.08
H3C3	1.09	1.09	H3C2	1.08	1.08
C2C1	1.50	1.49	C3C2	3.04	3.11
N2C2	1.15	1.15	N2C3	1.16	1.17
C3C1N1	128.0	127.0	C2C1X1	90.0	90.0
H1C3C1	107.5	107.6	H1C2C1	111.9	112.0
H2C3C1	111.8	112.3	H2C2C1	111.9	112.0
H3C3C1	111.8	112.3	H3C2C1	111.9	112.0
C2C1N1	123.1	121.8	C3C2X2	90.0	90.0
N2C2X	87.7	88.1	N2C3X3	90.0	90.0
H1C3C1N1	0.0861	0.0860	C2C1X1N1	180.0	180.0
H2C3C1N1	119.7	119.7	H1C2C1X1	0.000	0.000
H3C3C1N1	-119.5	-119.5	H2C2C1X1	120.0	120.0
C2C1N1C3	180.0	180.0	H3C2C1X1	-120.0	-120.0
N2C2XC1	180.0	180.0	C3C2X2C1	180.0	180.0
XC2	* 1.00	* 1.00	N2C3X3C2	180.0	180.0
XC2C1	* 90.0	* 90.0	X1C1	* 1.00	* 1.00
XC2C1N1	* 0.00	* 0.00	X1C1N1	* 90.0	* 90.0
			X2C2	* 1.00	* 1.00
			X2C2C1	* 90.0	* 90.0
			X2C2C1X1	* 0.000	* 0.00
			X3C3	* 1.00	* 1.00
			X3C3C2	* 90.0	* 90.0
			X3C3C2X2	* 0.000	* 0.000
E(3-21G)	-222.9205 a.u.			-222.9657 a.u.	
E(4-31G)		-223.8489 a.u.			-223.8875 a.u.

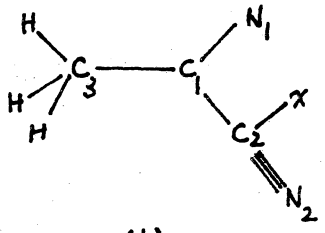

(1)

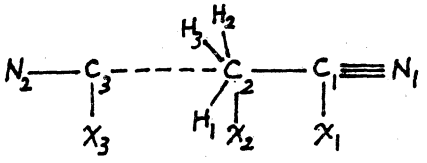

(3)

Table 14 Optimized Geometrical Parameters and Energy Values (continued)

Data with * are fixed parameters. Units in A or deg..

Ref. Structure			Monomer		
Basis set	3-21G	4-31G	Basis set	3-21G	4-31G
C1N1	1.14		C1N	1.14	
C2C1	1.46		C1C2	1.46	
HC	1.08		C2H1	1.08	
N2C3	1.17		C1C2H1	110.2	
HC2C1	110.3		XC1	* 1.00	
X1C1	* 1.00		XC1N	* 90.0	
X1C1N1	* 90.0		C2C1X	* 90.0	
C2C1X1	* 90.0		C2C1XN	* 180.0	
C2C1X1N1	* 180.0		H1C2C1X	* 0.000	
H1C2C1X1	* 0.000		H2C2C1X	* 120.0	
H2C2	HC		H3C2C1X	*-120.0	
H2C2C1	HC2C1		H2C2	C2H1	
H2C2C1X1	120.0		H3C2	C2H1	
H3C2	HC		H2C2C1	C1C2H1	
H3C2C1	HC2C1		H3C2C1	C1C2H1	
H3C2C1X1	*-120.0				
X2C2	* 1.00				
X2C2C1	* 90.0				
X2C2C1X1	* 0.00				
C3C2	* 8.00				
C3C2X2	* 90.0				
C3C2X2C1	* 180.0				
X3C3	* 1.00				
X3C3C2	* 90.0				
X3C3C2X2	* 0.00				
N2C3X3	* 90.0				
N2C3X3C2	* 180.0				
E(3-21G)	-222.9462 a.u.			-131.1918 a.u.	

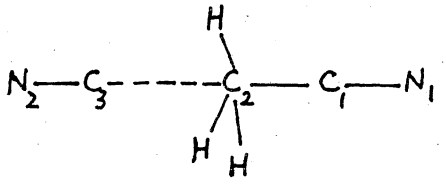

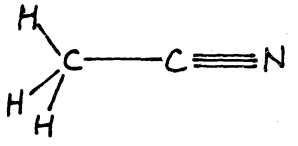

Table 14 Optimized Geometrical Parameters and Energy Values (continued)

Data with * are fixed parameters. Units in A or deg..

Structure 4			Structure 2		
Basis set	3-21G	4-31G	Basis set	3-21G	4-31G
C1N1	1.15	1.16	C1X1		0.69
C2C1	2.09	2.11	C2X1		0.69
H1C2	1.06	1.06	C3X1		2.23
H2C2	1.06	1.06	H1C3X1C1		-0.00
H3C2	1.06	1.06	H2C3X1C1		120.3
C3C2	2.09	2.11	H3C3X1C1		-120.3
N2C3	1.15	1.16	N1C1		* 1.16
C2C1X1	89.98	90.0	N1C1X1		* 165.3
H1C2C1	89.96	90.0	X2X1		* 1.00
H2C2C1	90.01	90.0	X2X1C1		* 90.0
H3C2C1	90.01	90.0	X2X1C1N1		* 180.0
C3C2H1	90.02	90.0	C2X1X2		* 90.0
N2C3X2	90.01	90.0	C2X1X2C1		* 180.0
C2C1X1N1	180.0	180.0	N2C2		* 1.16
H1C2C1X1	0.0	0.0	N2C2X1		* 165.3
H2C2C1X1	120.0	120.0	N2C2X1X2		* 180.0
H3C2C1X1	-120.0	-120.0	C3X1C1		* 90.0
C3C2H1C1	180.0	180.0	C3X1C1N1		* 180.0
N2C3X2C2	180.0	180.0	H1C3		* 1.09
X1C1	* 1.00	* 1.00	H1C3X1		* 108.9
X1C1N1	* 90.0	* 90.0	H2C3		* 1.09
X2C3	* 1.00	* 1.00	H2C3X1		* 108.9
X2C3C2	* 90.0	* 90.0	H3C3		* 1.09
X2C3C2H1	* 0.000	* 0.000	H3C3X1		* 108.9
E(3-21G)	-222.9043 a.u.				
E(4-31G)		-223.8178 a.u.			-223.7691 a.u.

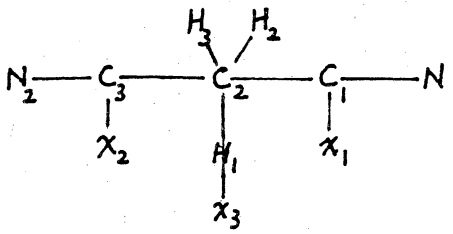

(4)

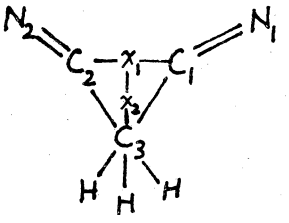

(2)

Table 14 Optimized Geometrical Parameters and Energy Values (continued)

Data with * are fixed parameters. Units in A or deg..

Structure 5			Structure 7		
Basis set	3-21G	4-31G	Basis set	3-21G	4-31G
C1N1	1.14	1.15	C1N1	* 1.21	1.23
C2C1	1.47	1.47	C2C1	* 1.41	1.43
C3C2	1.37	1.37	C3C2	* 1.51	1.51
H2C3	1.08	1.07	H2C3	1.09	1.08
H3C3	1.07	1.07	H3C3	* H2C3	1.08
N2C2	1.32	1.33	N2C2	* 1.27	1.26
H1N2	1.02	1.01	H1N2	1.03	1.02
C2C1X	89.75	90.3	C2C1N1	151.70	154.0
C3C2C1	113.24	114.1	C3C2C1	* 61.60	66.6
H2C3C2	120.7	120.6	H2C3C1	123.72	120.3
H3C3C2	121.4	121.7	H3C3C1	123.73	120.3
N2C2C1	112.0	112.2	N2C2C1	*152.60	151.4
H1N2C2	109.3	110.4	H1N2C2	111.36	112.1
C2C1XN1	180.0	180.0	C3C2C1N1	180.0	180.0
C3C2C1X	180.0	180.0	H2C3C1N1	*-90.0	-75.9
H2C3C2C1	180.0	180.0	H3C3C1N1	* 90.0	75.9
H3C3C2C1	0.000	0.000	N2C2C1N1	* 0.000	0.0204
N2C2C1X	0.000	0.000	H1N2C2C3	0.0058	0.0097
H1N2C2C1	180.0	180.0			
XC1	* 1.00	* 1.00			
XC1N1	* 90.0	* 90.0			
E(3-21G)	-222.9161 a.u.			-222.7979 a.u.	
E(4-31G)		-223.8446 a.u.			-223.7415 a.u.

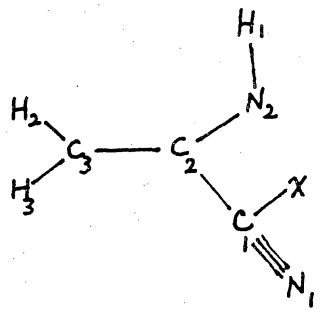

(5)

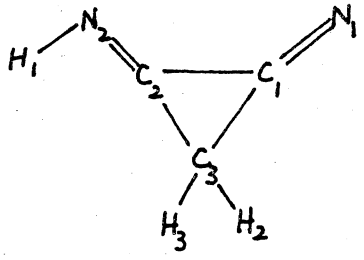

(7)

Table 15 Comparison of the energy levels using the various computational methods, kcal/mol

Activation Energies

	3-21G	4-31G	MNDO
Scheme 1 (1-2)		50.1	53.5
Scheme 3 (5-6)	> 74.2	> 54.7	43.0
Scheme 2 (3-4)	38.5	43.8	26.8

Stabilizing Energies

	3-21G	4-31G	MNDO
Cyanoacetaldimine anion (1)	16.1	12.0	-30.9
Transition State (2)		62.1	22.6
Cyanide anion-acetonitrile complex (3)	-12.2	-12.2	- 6.1
Transition State (4)	26.3	31.6	20.7
Cyanoacetaldimine anion (5)	18.9	14.7	-36.6
Transition State (6)			6.4
Cyclopropanedi-imine anion (7)	93.1	79.4	1.6

Energies in column 3-21G relative to Ref. structure in Table 14.
Energies in column 4-31G relative to TS (3) in colomn 3-21G.
Energy reference in MNDO colomn see Ref. 7.

Discussion

Based on our 4-31G results, the activation energy of the S_N 2 mechanism (scheme 2) is 43.8 kcal/mol. This is lower than the 54.7 kcal/mol energy difference between precusor (5) and intermediate (7) of scheme 3. The activation energy of scheme 3 must be larger than 54.7 kcal/mol as shown in Fig. 14.

The energy level of precusor (3) in the S_N2 mechanism, -12.2 kcal/mol (3-21G) is more stable than those of (1), + 12.0 kcal/mol and (5), + 14.7 kcal/mol (3-21G) respectively. Similar results are seen from the 4-31G results. Therefore, we conclude that the Walden inversion is the more likely mechanism based on both its activation energy and the stability energy levels of the precusors of scheme 1 and scheme 3 when either 3-21G or 4-31G energy levels are used. Comparison of the energy levels using the various computational methods is shown in Table 15.

Even though not all parameters of the transition structure 2 (scheme 1) were optimized in our 4-31G calculation, an approximate activation energy of scheme 1, 50.1 kcal/mol, was calculated and this suggests that the Walden inversion (scheme 2) predominants over the mechanism suggested by Jay et al.. Kinetic calculations using Andrades' MNDO results also show that the Walden inversion is more likely than the mechanism of scheme 1.

Contrary results were obtained for the relationship between the Walden inversion and the mechanism of scheme 3 from MNDO and 4-31G results as shown by kinetic estimation as well as by the stability energies of the precusors. However, the activation energies of the Walden inversion is the lowest in both cases. In fact, if the activation energy of the process from (1) to (5) is included, it shows that the mechanism of scheme 3 is even more unfavorable.

Based on this simplified kinetic estimation and our 4-31G results, we support the Walden inversion as the most likely mechanism among the three suggested. It should be noted, however, that solvent effects are not included in any of the theoretical calculations. Inclusion of solvation effects could alter the reaction mechanism which would be predicted.

Appendix A. Cartesian coordinates of the methanol crystal

Appendix A: Cartesian coordinates of the methanol crystal

The coordinates of C and O are based on Ref.45. Those of H are based on 6-31G* results. Those of the lone pairs are based upon the empirical potential. Units in Angstrom.

Digital symbols are the same as that in Ref. 18, where 1-C, 5-H, 6-O, 21-H (connected to O) and 20-lone pair. A, B, D, D', G are the methanol molecules shown in Fig. 11.

Lattice Energy calculated = -7.9 kcal/mol.

A	0.0	1.557230	1.167500	1A
	0.0	1.254371	0.120420	5A
	0.890004	1.164695	1.659341	5A
	-0.890004	1.164695	1.659341	5A
	0.0	2.977230	1.167500	6A
	0.000001	3.434656	1.996126	21A
	-0.459627	3.173264	0.835365	20A
	0.459627	3.173264	0.835364	20A
B	0.0	4.262770	3.502500	6B
	0.0	5.682770	3.502500	1B
	0.000001	3.805344	4.331126	21B
	0.0	5.985629	4.549580	5B
	0.890004	6.075305	3.010659	5B
	-0.890004	6.075305	3.010659	5B
	-0.459627	4.066736	3.834635	20B
	0.459627	4.066736	3.834636	20B
D	3.215	5.177230	1.167500	1D
	3.215	4.874371	0.120420	5D
	4.105004	4.784695	1.659341	5D
	2.324996	4.784695	1.659341	5D
	3.215	6.597230	1.167500	6D
	3.214999	7.054656	1.996126	21D
	2.755373	6.793264	0.835365	20D
	3.674627	6.793264	0.835364	20D
G	3.215	0.642770	3.502500	6G
	3.215	2.062770	3.502500	1G
	3.214999	0.185344	4.331126	21G
	3.215	2.365629	4.549580	5G
	4.105004	2.455305	3.010659	5G
	2.324996	2.455305	3.010659	5G
	2.755373	0.446736	3.834635	20G
	3.674627	0.446736	3.834636	20G
D'	3.215	-0.642770	1.167500	6D'
	3.215	-2.062770	1.167500	1D'
	3.214999	-0.185344	1.996126	21D'
	3.215	-2.365629	0.120420	5D'
	4.105004	-2.455305	1.659341	5D'
	2.324996	-2.455305	1.659341	5D'
	2.755373	0.446736	0.835365	20D'
	3.674627	0.446736	0.835364	20D'

References:

1. A. T. Hagler, E. Huler and S. Lifson, J. Am. Chem. Soc. 96, 5319, (1974).

2. W. L. Jorgensen, J. Am. Chem. Soc., 101, 2011 (1979); ibid, 101, 2016 (1979); ibid, 102, 3309 (1980); ibid, 102, 543 (1980); J. Chem. Phys. 71, 5034 (1979); J. Phys. Chem. 90, 6379 (1986).

3a. R. Taylor, J. Molecular Structure, 71, 311 (1981).
b. R. Taylor, J. Molecular Structure, 73, 125 (1981).

4. L. M. J. Kroon-Batenburg & J. A. Kanters, J. Molecular Structure, 105, 417 (1983).

5. A. Ben-Naim & F. H. Stillinger, in "Water and Aqueous Solutions", edited by R. A. Horne (Wiley, New York, 1972), p.295.

6. M. Jay, W. J. Layton and G. A. Digenis, Tetrahedron Letters, 21, 2621-4, (1980).

7. J. G. Andrade, T. Clark, J. Chandrasekhar & P. v. R. Schleyer, Tetrahedron Letters, 22, 2957-60, (1981).

8. K. Morokuma & L. Pedersen, J. Chem. Phys. 48, 3275 (1968).

9. J. Del. Bene & J. A. Pople, Chem. Phys letters, 4, 426 (1969). J. Del. Bene & J. A. Pople, J. Chem. Phys. 52, 4858 (1970).

10a P. A. Kollman & L. C. Allen, J. Chem. Phys., 52, 5085, (1970).
b P. A. Kollman & L. C. Allen, J. Am. Chem. Soc. 93, 4991, (1971).

11. D. G. Truhlar, "Potential Energy Surfaces and Dynamic Calculations for Chemical Reactions and Molecular Energy Transfer", Plenum Press, New York, N.Y.(1981).

12a W. L. Jorgensen & M. Ibrahim, J. Am. Chem. Soc., 102, 3309 (1980).
b W. L. Jorgensen, J. Phys. Chem., 90, 6379 (1986).

13. O. Matsuoka, E. Clementi & M. Yoshimine, J. Chem. Phys. 64, 1351 (1976).

14. A. Ben-Naim, "Water and Aqueous Solutions", Plenum Press, New York, 1974.

15. R. O'Neill, Appl. Statistics, 20, 338-345 (1971).

16. W. H. Stockmayer, J. Chem. Phys. 9, 398 (1941).

17a J. S. Rowlinson, Trans. Faraday Soc., 45, 974 (1949).
b J. S. Rowlinson, Trans. Faraday Soc., 47, 120 (1951).
c J. S. Rowlinson, J. Chem. Phys., 19, 827 (1951).

18a Quantum Chemistry Program Exchange, No. 318, Chemisry Department, Indiana University, Bloomington, IN.
b Quantum Chemistry Program Exchange, No. 395, Chemisry Department, Indiana University, Bloomington, IN.

19. H. Popkie, H. Kistenmacher & E. Clementi, J. Chem. Phys. 59, 1325 (1973).

20. J. D. Bernal & F. D. Fowler, J. Chem. Phys. 1, 515 (1933).

21. N. Bjerrum, Kgl. Danske Videnskab. Selskab, Mat.-Fys. Medd., 27, 1 (1951).

22. D. Eisenberg & W. Kauzmann, "The Structure and Properties of Water" (Oxford, U. P., New York. 1969), p. 139, 71.

23. T. Oie, G. M. Maggiora & R. E. Christoffersen, International J. of Quantum Chemistry: Quantum Biology Symposium 8, 1 (1981).

24. M. D. Newton, J. Phys. Chem. 87, 4288 (1983).

25. B. R. Lentz & H. A. Scheraga, J. Chem. Phys. 58, 5296 (1973); 61, 3493, (1974).

26. K. T. No & M. S. John, J. Phys. Chem. 87, 226 (1983).

27. D. Hankins, J. W. Moskowitz & F. H. Stillinger, J. Chem. Phys. 53, 4544 (1970).

28. T. R. Dyke, K. M. Mack & J. S. Muenter, J. Chem. Phys., 66, 498 (1977).

29. L. A. Curtiss, D. J. Frurip & M. Blander, J. Chem. Phys. 71, 2703 (1979).

30. H. A. Gebbie, W. J. Burroughs, J. Chamberlain, J. E. Harries & R. G. Jones, Nature 221, 143 (1969).

31. G. S. Kell, G. E. McLaurin, & E. Whalley, J. Chem. Phys. 48, 3805 (1968); ibid. 49, 2839 (1968); G. S. Kell & G. E. McLaurin, ibid. 51, 4345 (1969).

32. J. H. Dymond & E. B. Smith, The Virial Coefficients of Gases (Clarendon, Oxford, 1969); F. G. Keyes, J. Chem. Phys. 15, 602 (1947).

33. J. D. Lambert & E. D. T. Strong, Proc. R. Soc. London Ser. A. 200, 566 (1950).

34. J.E. Lowder, J. Quant. Spectrosc. Radiat. Transfer, 10, 1085 (1970).

35. G. G. Gimmestad & G. W. F. Pardow, J. Quant. Spectrosc. Radiat. transfer, 12, 559 (1972).

36. K. D. Cook & J. W. Taylor, Int. J. Mass Spectrosc. Ion Phys., 30, 345 (1979).

37. J. D. Dill, L. C. Allen, W. C. Topp & J. A. Pople, J. Am. Chem. Soc., 97, 7220 (1975).

38. G. Brink & L Glasser, J. Compt. Chem. 2, 177-181 (1981).

39. M. D. Newton, G. A. Jeffrey & S. Takagi, J. Am. Chem. Soc. 101, 1997 (1979).

40. L. Pauling, "The Nature of the Chemical Bond", Cornell University Press, Ithaca, New York, 1960, p467.

41. S. W. Peterson & H. A. Levy, Acta Cryst., 10, 70 (1957).

42. E. Whalley, "The Hydrogen Bond" Vol.III, pp1425-70, Edited by P. Schuster, G. Zundel & C. Sandorfy, North-Holland Publishing Company, 1976.

43. D. P. Santry, J. Am. Chem. Soc. 94, 8311 (1972).

44. R. M. Badger & S. H. Bauer, J. Chem Phys. 5, 839 (1937).

45. K. J. Tauer & W. N. Lipscomb, Acta Cryst., 5, 606 (1952).

46a W. L. Bragg, Proc. Roy. Soc. A105, 370-386 (1924).
b W. L. Bragg, ibid, A106, 346-368 (1924).

47. W. H. Zachariasen, J. Chem. Phys. 1, 640-642 (1933).

48a S. Bhagavantam, Proc. Roy. Soc. A124, 545-554 (1929).
b S. Bhagavantam, ibid, A126, 143-154 (1930).

49. M. M. Julian and F. D. Bloss, Acta Cryst. A38, 167-169 (1982).

50. C. W. Bunn, Chemical Crystallography. Oxford University Press, London (1961).

51. D. E. Sands, Vectors and Tensors in Crystallography. Addison-Wesley Publishing Co.,Massachusetts. p126 (1982).

52. J. F. Nye, Physical Properties of Crystals. Oxford University Press, London (1957).

53. J. Yoshimura, Y. Ohgo & T. Sato, Bull. Chem. Soc. Japan, 38, 1809 (1965).

54. "The Chemistry of the Cyano Group", Z. Rapoport, Ed., Chapter 6, Interscience Publishers, N.Y. (1970).

55a J. March, "Advanced Organic Chemistry: Reactions, Mechanisms and Structures", McGraw-Hill, N.Y. (1968) pp. 803 and 714.
b J. March, "Advanced Organic Chemistry: Reactions, Mechanisms and Structures", 2nd Ed., p.533, 962 McGraw Hill, N.Y. (1977).

56. R. B. Woodward & Hoffmann, Angew. Chem. Int. Ed. Engl., 10, 781 (1969).

57. P. D. Adeney, W. J. Bouma, L. Radom & W. R. Rodwell, J. Am. Chem. Soc., 102, 4069 (1980);
W. J. Bouma, D. Poppinger & L. Radom, J. Am. Chem. Soc., 99, 6443 (1977);
W. J. Bouma, M. A. Vincent & L. Radom, Int. J. Quantum Chem., 14, 767 (1978).

58. J. W. Viers, J. C. Schug & M. D. Stovall, J. Comput. Chem. 5, 598 (1984).
59. S. Wolfe, D. J. Mitchell & H. B. Schlegel, J. Am. Chem. Soc., 103, 7692 (1981); 103, 7694 (1981).

The vita has been removed from the scanned document